## ALGEBRAIC MULTIGRID METHODS FOR METRIC-PERTURBED COUPLED PROBLEMS\*

ANA BUDIŠA†, XIAOZHE HU‡, MIROSLAV KUCHTA†, KENT-ANDRE MARDAL $^{\S}$ , AND LUDMIL ZIKATANOV $^{\P}$ 

Abstract. We develop multilevel methods for interface-driven multiphysics problems that can be coupled across dimensions and where complexity and strength of the interface coupling deteriorates the performance of standard methods. We focus on aggregation-based algebraic multigrid methods with custom smoothers that preserve the coupling information on each coarse level. We prove that, with the proper choice of subspace splitting, we obtain uniform convergence in discretization and physical parameters in the two-level setting. Additionally, we show parameter robustness and scalability with regard to the number of the degrees of freedom of the system on several numerical examples related to the biophysical processes in the brain, namely, the electric signaling in excitable tissue modeled by bidomain, the extracellular-membrane-intracellular (EMI) model, and reduced EMI equations.

**Key words.** algebraic multigrid method, preconditioning, iterative method, coupled problems, graph Laplacian

MSC codes. 65F08, 65N55, 65S05

**DOI.** 10.1137/23M1572076



See reproducibility of computational results at end of the article.

**1. Introduction.** In this paper, we consider multilevel methods for a family of coupled problems of the following form: Find  $u_{\Omega} \in V(\Omega)$ ,  $u_{\Upsilon} \in V(\Upsilon)$  such that

$$(1.1) \qquad \left(\begin{pmatrix} A_{\Omega} & \\ & A_{\Upsilon} \end{pmatrix} + \gamma \begin{pmatrix} -\sigma'_{\Omega} \\ \sigma'_{\Upsilon} \end{pmatrix} \begin{pmatrix} -\sigma_{\Omega} & \sigma_{\Upsilon} \end{pmatrix} \right) \begin{pmatrix} u_{\Omega} \\ u_{\Upsilon} \end{pmatrix} = \begin{pmatrix} f_{\Omega} \\ f_{\Upsilon} \end{pmatrix}.$$

Here,  $A_{\iota}: V(\Omega_{\iota}) \to V(\Omega_{\iota})', \iota = \Omega, \Upsilon$  are elliptic and decoupled operators, while the coupling on the common interface  $\Gamma = \overline{\Omega} \cap \overline{\Upsilon}$  is represented by the interface operator  $R = (-\sigma_{\Omega} \quad \sigma_{\Upsilon}): V(\Omega) \times V(\Upsilon) \to V(\Gamma)'$ . We refer to the coupling term R'R as the metric term since, by assumption, the coupling is a symmetric and semidefinite operator. In fact, R is typically either an identity or a projection operator which in the limit  $\gamma \to \infty$  enforces a coupling between  $u_{\Omega}$  and  $u_{\Upsilon}$  either in the whole domain or on parts of it. As  $A_{\Omega}$  and  $A_{\Upsilon}$  are elliptic, multilevel methods for these operators are readily available as solvers, but performance is typically lost for large  $\gamma$ . The topic of this paper is to adapt the multilevel algorithms such that they are robust with respect to  $\gamma$ .

A1461

<sup>\*</sup>Submitted to the journal's Numerical Algorithms for Scientific Computing section May 10, 2023; accepted for publication (in revised form) January 22, 2024; published electronically May 2, 2024. https://doi.org/10.1137/23M1572076

Funding: The first and fourth authors acknowledge financial support funded by the Norwegian Research Council (grant 102155). The work of the second author is partially supported by the National Science Foundation (grant DMS-2208267). The third author acknowledges support from the Norwegian Research Council (grant 303362). The research of the fifth author is supported in part by the U.S.-Norway Fulbright Foundation and the National Science Foundation (grant DMS-2208249).

<sup>†</sup>Simula Research Laboratory, 0164 Oslo, Norway (ana@simula.no, miroslav@simula.no).

<sup>&</sup>lt;sup>‡</sup>Department of Mathematics, Tufts University, Medford, MA 02155 USA (xiaozhe.hu@tufts.edu). §Simula Research Laboratory, 0164 Oslo, Norway, and Department of Mathematics, University of Oslo, Blindern, 0316 Oslo, Norway (kent-and@uio.no).

<sup>&</sup>lt;sup>¶</sup>Department of Mathematics, Pennsylvania State University, University Park, PA 16802 USA (ludmil02@gmail.com).

The abstract problem arises in many multicompartment, multiphysics, and multiscale applications. For multicompartment problems, a common approach is to consider the system in terms of its blocks and adapt appropriate block preconditioners. Examples are the bidomain equations [51, 42] in cardiac modeling and multiplenetwork poroelasticity problems [23, 24, 10, 46, 45] in porous media modeling. The block approach has been quite successful, and in most situations, parameter-robust solution algorithms have been found. Arguably, a more challenging family of problems are the multiphysics problems coupled through a common interface, which is a manifold of codimension one. For some but not all of these problems, metric terms at the interface arise. Examples are the so-called extracellular-membrane-intracellular (EMI) model of excitable tissue [1, 50, 55] and the Biot-Stokes coupled problems [3]. Finally, certain multiscale problems are interface coupled problems in which dimensionality of one of the subproblems is reduced by model reduction techniques. Here, the examples are the three-dimensional/one-dimensional problem of tissue perfusion [13] or well-block pressure in reservoir simulations [43]. In particular, for tissue perfusion modeling of whole-brain vasculature corresponding to tens of millions vessels in mice and tens of billions vessels in humans [38], simulations are a major challenge, and one-dimensional representation of the vascular networks is a reasonable assumption.

Multigrid methods for singularly perturbed problems have been considered in several settings. Examples include discretizations of the linear elasticity equations in primal form [48] or H(div) and H(curl) problems [2]. Furthermore, the methods were generalized to algebraic multilevel methods (AMG) in [35, 36, 37]. A crucial observation is that the kernel or the near kernel must be carefully treated, or else the performance of the method deteriorates when the coupling parameter  $\gamma$  increases. We apply this observation to the abstract problem (1.1). In our setting, we study three cases where (1)  $\Omega_1 = \Omega_2$ , (2)  $\Omega_1$  and  $\Omega_2$  share a common interface of codimension one, and (3)  $\Omega_2$  is a lower-dimensional manifold of codimension two embedded in  $\Omega_1$ . We also consider the case where the meshes of  $\Omega_1$ ,  $\Omega_2$  and their interface are not nested.

The paper is organized as follows. After section 2, where motivating applications are presented, we state our main results in section 3. Experimental results showcasing robustness of the developed multgrid method are given in section 4. We finally draw conclusions in section 5.

- **2. Examples.** To motivate the computational method developed in this paper, we first provide several practical examples which fit the template of the abstract problem (1.1).
- **2.1. Bidomain model.** An example of a multicompartment problem are the so-called bidomain equations used to model the electrical activity of the heart [54]. It is a system of nonlinear ODEs and PDEs typically solved using an operator-splitting approach to solve ODE and PDE parts separately; cf. the overviews [17, 51]. Let  $\Omega$  be the homogenized tissue, and assume that the source terms  $f_e, f_i : \Omega \to \mathbb{R}$  and conductivities  $\alpha_e, \alpha_i > 0$  are given, with indices e and i representing extracellular and intracellular parts, respectively. Then, at each PDE time step, one seeks extracellular  $u_e : \Omega \to \mathbb{R}$  and intracellular  $u_i : \Omega \to \mathbb{R}$  potentials such that

(2.1a) 
$$-\nabla \cdot (\alpha_e \nabla u_e) + \gamma (u_e - u_i) = f_e \quad \text{in } \Omega,$$

(2.1b) 
$$-\nabla \cdot (\alpha_i \nabla u_i) + \gamma (u_i - u_e) = f_i \quad \text{in } \Omega.$$

Here,  $\gamma$  relates inversely to the time step size, and suitable boundary conditions are assigned. Efficient methods for the formulation of bidomain equations in terms of

 $u_i$  or  $u_e$  and the so-called transmembrane potential  $u_i - u_e$  have been developed by, e.g., [15, 44, 52, 28, 62]. We focus on the formulation (2.1) with unknown intra- and extracellular potentials.

To solve the equations (2.1), we discretize the system using the finite element method (FEM). Denote with  $L^2 = L^2(\Omega)$  the function space of square-integrable functions on  $\Omega$  and  $H^s = H^s(\Omega)$  the Sobolev spaces with s derivatives in  $L^2$ . Furthermore, let  $V \subset H^1(\Omega)$  be the discretization by continuous linear finite elements ( $\mathbb{P}_1$ ). The discrete variational formulation states to find  $u_e, u_i \in V$  such that for  $f_e, f_i \in V'$ ,

$$(2.2) \qquad \left( \begin{pmatrix} -\alpha_e \Delta \\ -\alpha_i \Delta \end{pmatrix} + \gamma \begin{pmatrix} I & -I \\ -I & I \end{pmatrix} \right) \begin{pmatrix} u_e \\ u_i \end{pmatrix} = \begin{pmatrix} f_e \\ f_i \end{pmatrix}.$$

We see that for  $\gamma > 0$ , the system is symmetric positive definite. However, it contains a singular strongly weighted lower-order term for which the kernel functions  $(v_e, v_i) \in V \times V$  are such that  $v_e = v_i$ . It is clear that the kernel contains both high- and low-frequency components, making it critical to handle the kernel with a multilevel algorithm [35].

**2.2. EMI model.** The modeling assumption of the coexistence of the interstitium, extracellular space, and the cell membrane, which is at the core of the bidomain system (2.1), has recently been challenged by the EMI models [1, 55] (also known as cell-by-cell models [27]). In the EMI model, the geometry of each compartment is resolved explicitly, which leads to a coupled mixed-dimensional problem posed on d-dimensional domains  $\Omega_i \subset \Omega_e$  separated by the interface  $\Gamma = \overline{\partial \Omega_i} \cap \overline{\partial \Omega_e}$ , which is a manifold of codimension one. Following the operator-splitting approach as in subsection 2.1, the PDE step now solves

(2.3a) 
$$-\nabla \cdot (\alpha_e \nabla u_e) = 0 \qquad \text{in } \Omega_e,$$

(2.3b) 
$$-\nabla \cdot (\alpha_i \nabla u_i) = 0 \quad \text{in } \Omega_i,$$

$$(2.3c) \alpha_i \nabla u_i \cdot \nu_i + \alpha_e \nabla u_e \cdot \nu_e = 0 on \Gamma,$$

(2.3d) 
$$\gamma(u_i - u_e) + \alpha_i \nabla u_i \cdot \nu_i = f \qquad \text{on } \Gamma.$$

Here, f is the source term coming from the ODE part, and  $\nu_{\iota}$  is the normal vector on  $\Gamma$  pointing outward with respect to  $\Omega_{\iota}$ ,  $\iota \in \{i, e\}$ . The system is typically equipped with homogeneous Neumann conditions on  $\partial \Omega_{e}$ . We remark that in (2.3), we assumed, for simplicity, that  $\Omega_{e}$  contains only a single cell/intracellular domain.

Variational formulation of (2.3) posed in  $V_e \times V_i$  with  $V_e = H^1(\Omega_e)$ ,  $V_i = H^1(\Omega_i)$  gives rise to a problem,

(2.4) 
$$\begin{pmatrix} -\alpha_e \Delta & \\ & -\alpha_i \Delta \end{pmatrix} + \gamma \begin{pmatrix} \tau'_e \tau_e & -\tau'_e \tau_i \\ -\tau'_i \tau_e & \tau'_i \tau_i \end{pmatrix} \begin{pmatrix} u_e \\ u_i \end{pmatrix} = \begin{pmatrix} f_e \\ f_i \end{pmatrix},$$

where the perturbation involves trace operators  $\tau_{\iota}$  such that  $\tau_{\iota}v_{\iota} = v_{\iota}|_{\Gamma}$  for  $\iota \in \{i, e\}$  and  $v_{\iota}$  is a continuous function on the respective domain. We observe that the EMI model (2.3) formulated in terms of intra- and extracellular potentials takes the form of the abstract problem (1.1), where, in particular, the perturbation operator induces  $(u_e, u_i) \mapsto \int_{\Gamma} (u_i - u_e)^2$ . Robust domain decomposition solvers for (2.4) have recently been developed in [27].

2.3. Reduced three-dimensional/one-dimensional EMI model. In a number of applications in geoscience (e.g., resorvoir simulations) and biomechanics (e.g., microcirculation), the EMI model (2.3) is applied in a geometrical setup where the domain  $\Omega_i$  is large but slender such that its resolution as a three-dimensional structure

by a computational mesh is impractical. This issue is addressed by model reduction which results in a one-dimensional representation of  $\Omega_i$  by a smooth (centerline) curve  $\Gamma$ . In [13], a mathematical formulation of a three-dimensional/one-dimensional coupled problem with application to tissue perfusion was analyzed. The numerical approximation of the problem has been a topic of many subsequent works; see, e.g., [18, 22, 34, 30, 32]. It includes, in particular, the challenge of traces of codimension two for standard elliptic problems which are not well-defined on  $H^1(\Omega)$ ,  $\Omega = \Omega_i \cup \Omega_e$ . Relatively few works have considered preconditioners for such problems [25, 33, 9].

To fit into the abstract setting of (1.1), we consider here a reduced EMI problem [34]: Find  $u_e \in H^1(\Omega)$ ,  $u_i \in H^1(\Gamma)$  such that

$$(2.5) \qquad \qquad \left( \begin{pmatrix} -\alpha_e \Delta \\ -\alpha_i \Delta \end{pmatrix} + \gamma \begin{pmatrix} \Pi_\rho' \Pi_\rho & -\Pi_\rho' \\ -\Pi_\rho & I \end{pmatrix} \right) \begin{pmatrix} u_e \\ u_i \end{pmatrix} = \begin{pmatrix} f_e \\ f_i \end{pmatrix}.$$

Here,  $\Pi_{\rho}$  is the averaging operator reducing  $u \in H^1(\Omega)$  to  $\Gamma$  by computing the function's average over a virtual cylinder with radius  $\rho$  which approximates the domain  $\Omega_i$ . More precisely, we let

$$(2.6) \qquad (\Pi_{\rho}u)(x) = \frac{1}{|C^{\nu}_{\rho}(x)|} \int_{C^{\nu}_{\rho}(x)} u, \qquad u \in H^{1}(\Omega),$$

where  $x \in \Gamma$ ,  $C^{\nu}_{\rho}(x)$  is a circle of radius  $\rho(x)$  in the plane with a normal  $\nu = \frac{\mathrm{d}\Gamma}{\mathrm{d}s}(x)$ , and s is the arc-length coordinate of  $\Gamma$ . Furthermore, for a smooth function v on  $\Gamma$ , we define  $\Delta v = \frac{\mathrm{d}^2 v}{\mathrm{d}s^2}$ .

We remark that the perturbation operator in (2.5) is symmetric, while the formulations [18, 13] utilize a standard trace operator in the coupling (in addition to  $\Pi_{\rho}$ ), leading to a nonsymmetric coupling term. Let us finally stress that (2.5) is typically only a component in advanced models that include convection and other processes; cf. [19, 21].

- 3. Two-level AMG for metric-perturbed coupled problems. In this section, we first reformulate the example systems of PDEs into a more general setting. This allows us to introduce aggregation-based AMG methods to solve our examples, as they are a general class of methods that can be used to solve a wide variety of PDE systems. We then prove the uniform convergence of the two-level AMG method under certain assumptions on the underlying subspace decomposition. These assumptions are shown to be sufficient and suitable for the problems we consider.
- **3.1. Preliminaries.** In the following, we slightly change the notation introduced in (1.1) by collecting all elliptic terms in a common bilinear form  $a_1$ , while another bilinear form  $a_0$  contains the metric terms. Specifically, let  $\Omega \subset \mathbb{R}^{d_{\Omega}}$ ,  $\Upsilon \subset \mathbb{R}^{d_{\Upsilon}}$ , and  $\Gamma \subset \mathbb{R}^{d_{\Gamma}}$  such that  $0 < d_{\Gamma} \le d_{\Omega}$ ,  $d_{\Upsilon} \le 3$ ,  $\overline{\Omega} \cap \overline{\Upsilon} \ne \emptyset$ , and  $\overline{\Gamma} \subset \overline{\Upsilon}$ . On each of the domains, we introduce quasi-uniform triangulation and a corresponding finite element space  $V_i$ ,  $i \in \{\Omega, \Upsilon, \Gamma\}$  with  $V_{\Gamma} \subseteq V_{\Upsilon}$ . For  $V = V_{\Omega} \times V_{\Upsilon}$ , we then consider bilinear forms  $a_0(\cdot, \cdot), a_1(\cdot, \cdot) : V \times V \to \mathbb{R}$  defined as

(3.1a) 
$$a_0((u_{\Omega}, u_{\Upsilon}), (v_{\Omega}, v_{\Upsilon})) = m_{\Gamma}(R(u_{\Omega}, u_{\Upsilon}), R(v_{\Omega}, v_{\Upsilon})),$$

(3.1b) 
$$a_1((u_{\Omega}, u_{\Upsilon}), (v_{\Omega}, v_{\Upsilon})) = a_{\Omega}(u_{\Omega}, v_{\Omega}) + a_{\Upsilon}(u_{\Upsilon \setminus \Gamma}, v_{\Upsilon \setminus \Gamma}) + a_{\Gamma}(u_{\Gamma}, v_{\Gamma})$$

for  $v_{\Upsilon} = (v_{\Upsilon \setminus \Gamma}, v_{\Gamma})$  and  $v_{\Gamma} \in V_{\Gamma}$ . Here,  $a_{\Omega}(\cdot, \cdot)$ ,  $a_{\Upsilon}(\cdot, \cdot)$ , and  $a_{\Gamma}(\cdot, \cdot)$  are bilinear forms corresponding to the elliptic equations, such as  $d_{\Omega}$ -,  $d_{\Upsilon}$ -, and  $d_{\Gamma}$ -Laplacians on their respective domains. The bilinear form  $m_{\Gamma}(\cdot, \cdot)$  is a lower-order (mass) term in  $V_{\Gamma}$ .

The interface operator  $R: V \to V'_{\Gamma}$  defines a metric on the interface; that is, for  $v = (v_{\Omega}, v_{\Upsilon}) \in V$ ,

$$(3.2) Rv = v_{\Gamma} - \sigma(v_{\Omega}),$$

where  $\sigma: V_{\Omega} \to V'_{\Gamma}$  is a linear restriction operator. In particular, we assume that  $\sigma$  is surjective and bounded, i.e.,  $\|\sigma(v_{\Omega})\|_{L^{2}(\Gamma)} \lesssim \|v_{\Omega}\|_{V_{\Omega}}$ . The main problem we want to solve is to find  $u \in V$  such that

(3.3) 
$$a(u,v) = \gamma a_0(u,v) + a_1(u,v) = f(v) \quad \forall v \in V,$$

where  $f \in V'$  and  $\gamma \gg 1$  is a coupling parameter.

Finally, we can define operators representing the bilinear forms in (3.1). Let  $A, A_0, A_1: V \to V'$  such that  $\langle A_0 u, v \rangle = a_0(u, v), \ \langle A_1 u, v \rangle = a_1(u, v), \ \text{and} \ A = \gamma A_0 + A_1$  for  $u, v \in V$ . Here,  $\langle \cdot, \cdot \rangle$  is the duality pairing between V and its dual V'. Additionally, let  $\|v\|_{\tilde{A}}^2 = \langle \tilde{A}v, v \rangle$  denote the  $\tilde{A}$ -norm of v for any symmetric positive definite operator  $\tilde{A}$  on V and  $v \in V$ . If  $\tilde{A}$  is only positive semidefinite,  $|v|_{\tilde{A}}^2 = \langle \tilde{A}v, v \rangle$  defines the  $\tilde{A}$ -seminorm. Equivalently to (3.3), we want to find  $u \in V$  such that

$$(3.4) \qquad \langle Au, v \rangle = \gamma \langle A_0u, v \rangle + \langle A_1u, v \rangle = \langle f, v \rangle \qquad \forall v \in V$$

We refer to this system as the *metric-perturbed coupled problem* since it is perturbed by a lower-order term  $A_0$  that can dominate the system when  $\gamma \gg 1$ .

Remark 3.1. In general, the interface operator (3.2) can be represented as  $R = (-\sigma_{\Omega} \quad \sigma_{\Upsilon})$ , where  $\sigma_{\Omega}$  and  $\sigma_{\Upsilon}$  are linear restriction operators (trace or averaging) on  $\Gamma = \overline{\Omega} \cap \overline{\Upsilon}$ . This generality would represent the case of nonconforming meshes between each subdomain  $\Omega$  and  $\Upsilon$  and their interface  $\Gamma$ . For example, in the EMI model (2.3),  $\sigma_i$  are the respective trace operators  $\sigma_{\iota}(v) = v_{\iota}|_{\Gamma}$ ,  $\iota \in {\Omega, \Upsilon}$ . However, we assume that at least one of the triangulations of subdomains, namely,  $\Upsilon$ , conforms to the interface (such that  $V_{\Gamma} \subseteq V_{\Upsilon}$ ) and that the restriction operator becomes of form  $\sigma_{\Upsilon} = (I_{\Gamma} \quad 0_{\Upsilon \setminus \Gamma})$ .

That implied, we see that the subdomain part  $\Upsilon \setminus \Gamma$  does not contribute to the metric coupling term  $a_0(\cdot,\cdot)$ . Therefore, the component of functions in  $V_{\Upsilon}$  defined only on  $\Upsilon \setminus \Gamma$  will not influence the convergence of the AMG method with regard to parameter  $\gamma$  and can be smoothed using standard methods, such as the Gauss–Seidel or the Jacobi method.

Hence, to simplify the exposition of the convergence theory, we will consider only the case when  $V_{\Gamma} = V_{\Upsilon}$  further in this paper. For example, in the reduced three-dimensional/one-dimensional EMI model (2.5), we have that  $\Upsilon = \Gamma$  is a curve in  $\Omega \subset \mathbb{R}^3$ ,  $\sigma_{\Omega}$  is the averaging operator (2.6), and  $\sigma_{\Upsilon}$  is the identity map. Note that for the bidomain model (2.1), we have  $\Omega = \Upsilon = \Gamma$  and that the restriction operators are simply identities.

Remark 3.2. By assumptions of ellipticity of  $A_1$  and boundedness of the restriction operators in the  $A_1$ -induced norm on V, the equivalence

$$\|v\|_{A_1}^2 \leq \langle Av, v \rangle \lesssim \gamma \|v\|_{A_1}^2 \quad \forall v \in V$$

holds, and we observe that the upper bound depends on  $\gamma$ . That is, preconditioning strategies based on the block-diagonal operator  $A_1$  (e.g., AMG with pointwise smoothers) cannot be robust in the coupling parameter.

In the following, we slightly abuse the notation and consider A,  $A_1$ , and  $A_0$  to be matrices and  $u_{\Omega}$  and  $u_{\Gamma}$  to be vectors that we obtain from a choice of an FEM basis, such as the linear continuous finite elements ( $\mathbb{P}_1$  elements). We present theoretical results based on reformulating the problem in terms of graph Laplacians.

To do so, we introduce the undirected graph  $\mathcal{G}(A)$  associated with the sparsity pattern of the symmetric positive definite matrix A. The vertices of  $\mathcal{G}(A)$  are labeled as  $\mathcal{V} = \{1, 2, \dots, N\}$ , where N represents the number of degrees of freedom (DOFs) of V. We use  $\mathcal{E}$  to denote the collection of edges e = (i,j) if  $(A)_{ij} \neq 0$ , with an intrinsic ordering. Specifically, we order any graph edge e = (i, j) with j < i for  $i, j \in \mathcal{V}$ . It is worth noting that the following equivalences are well known:

- 1. In the context of FEMs, mass matrices represent the matrix form of the  $L^2$ inner product on a portion or the entirety of the domain and are equivalent to diagonal matrices, as shown in [58]. For instance, this equivalence holds for  $\mathbb{P}_k$  elements, where the constants depend only on the polynomial order k. On the other hand, stiffness matrices, which correspond to second-order elliptic operators such as  $A_1$ , are spectrally equivalent to weighted graph Laplacians. We provide a sketch of the proof in Appendix A using results from [61, Lemma
- **2.** If  $\widetilde{A}: V \to V'$  is any positive semidefinite matrix and  $\widetilde{D}$  its diagonal, then we have

$$(3.5) ||v||_{\widetilde{A}}^2 \lesssim ||v||_{\widetilde{D}}^2 v \in V.$$

The constants hidden in this estimate depend on the number of nonzeros per row in A. The estimate is easily derived using the Schwarz inequality.

3. In particular, for any graph Laplacian on V, the following Poincaré inequality holds:

$$\inf_{c\in\mathbb{R}}\|v-c\mathbb{1}\|_{\widetilde{D}}^2\lesssim \|v\|_{\widetilde{A}}^2 \qquad v\in V.$$

The constants are determined by the weights in  $\widetilde{A}$  and are proportional to the square of the number of vertices in the graph divided by the square of the size of the minimal cut in the graph. The complete proof can be found, for example, in [49]. This result is used only locally for small size graphs, namely, on each aggregate that represents the coarse scale DOF in the two-level AMG method.

Consequently, the bilinear forms from (3.1) can be replaced by their equivalent graph forms. Let  $\mathcal{V} = \mathcal{V}_{\Omega} \cup \mathcal{V}_{\Gamma}$  be the division of graph vertices into two subsets with regard to discretizations of  $\Omega$  and  $\Gamma$ , respectively. Similarly, let  $\mathcal{E} = \mathcal{E}_{\Omega} \cup \mathcal{E}_{\Gamma}$ . Then, for  $u = (u_{\Omega}, u_{\Gamma}) \in V$  and  $v = (v_{\Omega}, v_{\Gamma}) \in V$ , we get

(3.7a) 
$$a_{\Omega}(u_{\Omega}, v_{\Omega}) = \sum_{e} \omega_{e} \, \delta_{e} u_{\Omega} \, \delta_{e} v_{\Omega},$$

(3.7a) 
$$a_{\Omega}(u_{\Omega}, v_{\Omega}) \approx \sum_{e \in \mathcal{E}_{\Omega}} \omega_{e} \, \delta_{e} u_{\Omega} \, \delta_{e} v_{\Omega},$$
(3.7b) 
$$a_{\Gamma}(u_{\Gamma}, v_{\Gamma}) \approx \sum_{e \in \mathcal{E}_{\Gamma}} \omega_{e} \, \delta_{e} u_{\Gamma} \, \delta_{e} v_{\Gamma},$$

(3.7c) 
$$a_0(u,v) \approx \sum_{k=1}^{N_{\Gamma}} m_k \left( u_{\Gamma,k} - (\sigma(u_{\Omega}))_k \right) \left( v_{\Gamma,k} - (\sigma(v_{\Omega}))_k \right),$$

$$\delta_e v = v_i - v_j, \quad e = (i,j), \quad \omega_e = \omega_{ij} > 0, \quad j < i,$$

where  $N_{\iota} = \dim V_{\iota}$ ,  $\iota \in \{\Omega, \Gamma\}$ . The weights  $\omega_{e}$  depend on the shape regularity of the mesh, and their behavior is as  $h^{d-2}$  if they correspond to a d-homogeneous simplicial complex, where h is the mesh size parameter. The elements  $m_{k}$  behave like  $h^{d_{\Gamma}}$  if  $\Gamma$  corresponds to a  $d_{\Gamma}$ -homogeneous simplicial complex. In the following section, we design aggregation-based AMG methods with special Schwarz smoothers to solve (3.4). For that, we use the above equivalences for the bilinear forms to prove that this AMG method satisfies the kernel and stability conditions that guarantee uniform convergence. The basic algorithms for constructing AMG hierarchies via unsmoothed and smoothed aggregation are introduced in [56, section 5.1]. Later, the adaptive versions of such methods were developed in [5]. Details about aggregation AMG based on matching in graphs also used in our algorithms are found in [11, 12, 29, 39].

**3.2.** Convergence of the two-level AMG. The main idea of any algebraic multigrid method is to construct a hierarchy of nested vector spaces, each of which targets different error components for the solution of (3.4). In the case of aggregation-based AMG methods, such as unsmoothed aggregation AMG (UA-AMG) and smoothed aggregation AMG (SA-AMG), there is an added advantage in that multiple approximations of near-kernel components of the matrix describing the linear system can be retained as elements of each subspace in the hierarchy. To illustrate this, we first introduce the necessary ingredients of AMG in the context of subspace correction methods [36, 59, 60].

Let us introduce the decomposition  $V = V_c + \sum_{j=1}^J V_j$ , where  $V_c \subset V$  and  $V_j \subset V$ , j = 1, ..., J. Then the AMG preconditioner associated with such subspace splitting for the system (3.4) is defined as

(3.8a) 
$$B = P_c + S$$
,  $S = \sum_{j=1}^{J} P_j$ , where

(3.8b)

$$\langle S^{-1}w, w \rangle = \inf \left\{ \sum_{j=1}^{J} \|w_j\|_A^2 : w = \sum_{j=1}^{J} w_j \text{ and } w_j \in V_j, j = 1, \dots, J \right\},$$

(3.8c)

$$\langle B^{-1}v, v \rangle = \inf \left\{ \|v_c\|_A^2 + \sum_{j=1}^J \|v_j\|_A^2 : v = v_c + \sum_{j=1}^J v_j \text{ and } v_c \in V_c, v_j \in V_j, 1, \dots, J \right\},$$

where  $P_j$  are the A-orthogonal projections on  $V_j$  for j = 1, ..., J. Here,  $V_c$  accounts for the correction on a coarse (sub)space, while  $V_j$  for  $j \ge 1$  define a Schwarz-type smoother on the fine grid.

Choosing the appropriate subspace decomposition is the essence of a robust and efficient preconditioner for the system (3.4). Therefore, we want to show that, within certain assumptions, B is a uniform preconditioner for A with regard to coupling parameter  $\gamma$  and mesh parameter h. The assumptions required in the convergence analysis are as follows:

(I) **Kernel decomposition condition**: Find the subspace decomposition  $V_j$  for j = 1, ..., J such that

(3.9) 
$$\operatorname{Ker}(A_0) = \operatorname{Ker}(A_0) \cap V_c + \sum_{j=1}^{J} \operatorname{Ker}(A_0) \cap V_j.$$

(II) **Stable decomposition condition**: For a given  $v \in V$ , there exist a splitting  $\{v_c\} \cup \{v_j\}_{j=1}^J$ ,  $v_c \in V_c$ , and  $v_j \in V_j$  such that

$$(3.10) ||v_c||_{A_1}^2 + \sum_{j=1}^J ||v_j||_{A_1}^2 \lesssim ||v||_{A_1}^2, ||v_c||_{A_0}^2 + \sum_{j=1}^J ||v_j||_{A_0}^2 \lesssim |v||_{A_0}^2.$$

Specifically, the subspace splitting of V defines a Schwarz preconditioner that uniformly bounds the condition number of the preconditioned system in  $\gamma$  if the kernel condition (3.9) is satisfied. Additionally, the uniform bound in h is guaranteed if for any  $v \in V$ , we construct an aggregate decomposition (coarse grid) stable in  $\|\cdot\|_{A_1}$  that is also stable in  $\|\cdot\|_{A_0}$ .

Remark 3.3. The kernel decomposition condition (3.9) usually fails for pointwise smoothers in the presence of metric terms. As illustration, we consider the bidomain equations where the kernel consists of functions of the form  $u_e(x) = u_i(x)$ ,  $x \in \Omega$ . If  $e_j$  is the jth coordinate vector, then a pointwise smoother only corrects in the one-dimensional space  $\operatorname{span}\{e_j\}$ . Clearly,  $\operatorname{Ker}(A_0) \cap \operatorname{span}\{e_j\} = \{0\}$ , as  $\operatorname{Ker}(A_0) = \operatorname{Range}\{\binom{I}{I}\}$ . This shows that the condition (3.9) does not hold, and, as seen from the numerical tests presented later, the method with a pointwise smoother is far from optimal with respect to the magnitude of the coupling parameter  $\gamma$ .

Assuming that these two conditions hold, we first show the main results on the condition number estimate of the system (3.4) preconditioned with B (3.8). More precisely, we show that the condition number  $\kappa(BA)$  of the preconditioned system (3.4) is bounded uniformly with respect to  $\gamma$  and h. Note that the orthogonal complement of  $\operatorname{Ker}(A_0)$  can be defined as

(3.11) 
$$\operatorname{Ker}(A_0)^{\perp} = \{ y \in V : \langle Ay, z \rangle = 0, \, \forall z \in \operatorname{Ker}(A_0) \}$$
$$= \{ y \in V : \langle A_1y, z \rangle = 0, \, \forall z \in \operatorname{Ker}(A_0) \},$$

and, similarly, we can define local kernels  $\operatorname{Ker}(A_0) \cap V_j$  and kernel complements  $\operatorname{Ker}(A_0)^{\perp} \cap V_j$  for  $j = c, 1, 2, \ldots, J$ . Furthermore, we define projections to local subspaces; that is, for any  $v \in V$ , let  $P_j : V \to V_j$ ,  $P_{1,j} : V \to V_j$ , and  $P_{0,j} : V \to \operatorname{Ker}(A_0)^{\perp} \cap V_j$  such that for all  $w_j \in V_j$ ,

(3.12) 
$$\langle A(P_{j}v), w_{j} \rangle = \langle Av, w_{j} \rangle, \\ \langle A_{1}(P_{1,j}v), w_{j} \rangle = \langle A_{1}v, w_{j} \rangle, \\ \langle A_{0}(P_{0,j}v), w_{j} \rangle = \langle A_{0}v, w_{j} \rangle.$$

for  $j=c,1,2,\ldots,J$ . These projections are referred to as elliptic projections. Since both A and  $A_1$  are nonsingular, the definitions of the elliptic projections  $P_j$  and  $P_{1,j}$  are standard, and their roles in practical domain decomposition and multigrid methods are discussed at length in classical references such as [4, 53]. Regarding the definition of  $P_{0,j}$ , for any  $v \in V$ , we have that  $P_{0,j}v$  is a unique element in  $\operatorname{Ker}(A_0)^{\perp} \cap V_j$  satisfying the third equation in (3.12) (see [36, 37] for more details).

With that defined, we can easily derive that for  $v \in V$  and v = y + z,  $z \in \text{Ker}(A_0)$  and  $y \in \text{Ker}(A_0)^{\perp}$ , it follows that

$$||v||_A^2 = ||y||_A^2 + ||z||_{A_1}^2.$$

The next lemma shows a triangle inequality for the projections defined in (3.12).

LEMMA 3.4. The following inequality holds for all  $v \in V$  and j = c, 1, 2, ..., J:

*Proof.* Since  $P_j v \in V_j$ , by the definitions of the projections, we have

$$\begin{split} \|P_{j}v\|_{A}^{2} &= \langle AP_{j}v, P_{j}v\rangle = \langle Av, P_{j}v\rangle = \gamma \langle A_{0}v, P_{j}v\rangle + \langle A_{1}v, P_{j}v\rangle \\ &= \gamma \langle A_{0}P_{0,j}v, P_{j}v\rangle + \langle A_{1}P_{1,j}v, P_{j}v\rangle \\ &\leq \frac{\gamma}{2} \left( \langle A_{0}P_{0,j}v, P_{0,j}v\rangle + \langle A_{0}P_{j}v, P_{j}v\rangle \right) + \frac{1}{2} \left( \langle A_{1}P_{1,j}v, P_{1,j}v\rangle + \langle A_{1}P_{j}v, P_{j}v\rangle \right) \\ &= \frac{\gamma}{2} \left| P_{0,j}v \right|_{A_{0}}^{2} + \frac{1}{2} \|P_{1,j}v\|_{A_{1}}^{2} + \frac{1}{2} \|P_{j}v\|_{A}^{2}. \end{split}$$

Moving the last term on the right to the left-hand side finishes the proof.

Using the previous lemma and definitions, we are ready to present the condition number estimate in the following theorem.

THEOREM 3.5. Let  $v = y + z \in V$  such that  $z \in \text{Ker}(A_0)$  and  $y \in \text{Ker}(A_0)^{\perp}$ , which is the orthogonal complement with regard to the  $A_1$ -inner product. Assuming that the conditions (3.9) and (3.10) hold, we get the estimate

(3.15) 
$$C_1 \le \frac{\langle B^{-1}v, v \rangle}{\|v\|_A^2} \le C_2 := 2 \left[ C_{\perp}(v) + C_0(v) \right],$$

where the constant  $C_1$  only depends on the maximum over the number of intersections between the subspaces  $V_j$ , j = 1, ..., J, and the constants  $C_{\perp}(v)$  and  $C_0(v)$  are

$$\begin{split} C_{\perp}(v) &= \inf_{y_c + \sum_{j=1}^J y_j = y} \left( \frac{|y_c|_{A_0}^2 + \sum_{j=1}^J |y_j|_{A_0}^2}{|y|_{A_0}^2} + \frac{\|y_c\|_{A_1}^2 + \sum_{j=1}^J \|y_j\|_{A_1}^2}{\|y\|_{A_1}^2} \right), \\ C_0(v) &= \inf_{z_c + \sum_{j=1}^J z_j = z} \frac{\|z_c\|_{A_1}^2 + \sum_{j=1}^J \|z_j\|_{A_1}^2}{\|z\|_{A_1}^2}. \end{split}$$

This implies that the condition number estimate is  $\kappa(BA) \leq C_2/C_1$ .

*Proof.* From the definition of  $B^{-1}$  in (3.8c), if  $v \in V$  and v = y + z with  $y \in \text{Ker}(A_0)^{\perp}$ ,  $z \in \text{Ker}(A_0)$ , we have that

$$\begin{split} &\left\langle B^{-1}v,v\right\rangle \\ &= \inf_{v_c + \sum_{j=1}^J v_j = v} \left( \|v_c\|_A^2 + \sum_{j=1}^J \|v_j\|_A^2 \right) \\ &\leq \inf_{y_c + \sum_{j=1}^J y_j = y; \ z_c + \sum_{j=1}^J z_j = z} \left( \|y_c + z_c\|_A^2 + \sum_{j=1}^J \|y_j + z_j\|_A^2 \right) \\ &\leq 2 \inf_{y_c + \sum_{j=1}^J y_j = y; \ z_c + \sum_{j=1}^J z_j = z} \left( \|y_c\|_A^2 + \|z_c\|_A^2 + \sum_{j=1}^J \left( \|y_j\|_A^2 + \|z_j\|_A^2 \right) \right) \\ &= 2 \inf_{y_c + \sum_{j=1}^J y_j = y} \left( \|y_c\|_A^2 + \sum_{j=1}^J \|y_j\|_A^2 \right) + 2 \inf_{z_c + \sum_{j=1}^J z_j = z} \left( \|z_c\|_{A_1}^2 + \sum_{j=1}^J \|z_j\|_{A_1}^2 \right). \end{split}$$

The first inequality above is a crucial inequality, as it follows from (1) the fact that the set of decompositions of v = y + z is larger than the set of decompositions of y and z (because any decomposition of y and z gives a decomposition of v) and (2) the kernel decomposition assumption (3.9), without which we cannot have a decomposition of  $z = z_c + \sum_{j=1}^{J} z_j$  with  $z_j \in \text{Ker}(A_0) \cap V_j$ , j = c, 1, 2, ..., J. Then, by using (3.13), we see that

$$\begin{split} \frac{\left\langle B^{-1}v,v\right\rangle}{\|v\|_{A}^{2}} &= \frac{\left\langle B^{-1}v,v\right\rangle}{\|y\|_{A}^{2} + \|z\|_{A_{1}}^{2}} \leq 2 \frac{\sum_{z_{c} + \sum_{j=1}^{J} z_{j} = z}^{\inf} \left( \|z_{c}\|_{A_{1}}^{2} + \sum_{j=1}^{J} \|z_{j}\|_{A_{1}}^{2} \right)}{\|y\|_{A}^{2} + \|z\|_{A_{1}}^{2}} \\ &+ 2 \frac{\inf_{y_{c} + \sum_{j=1}^{J} y_{j} = y}^{\int} \left( \|y_{c}\|_{A}^{2} + \sum_{j=1}^{J} \|y_{j}\|_{A}^{2} \right)}{\|y\|_{A}^{2} + \|z\|_{A_{1}}^{2}} \\ &\leq 2 \frac{\inf_{z_{c} + \sum_{j=1}^{J} z_{j} = z}^{\int} \left( \|z_{c}\|_{A_{1}}^{2} + \sum_{j=1}^{J} \|z_{j}\|_{A_{1}}^{2} \right)}{\|z\|_{A_{1}}^{2}} \\ &+ 2 \frac{\inf_{z_{c} + \sum_{j=1}^{J} y_{j} = y}^{\int} \left( \|y_{c}\|_{A}^{2} + \sum_{j=1}^{J} \|y_{j}\|_{A}^{2} \right)}{\gamma |y|_{A_{0}}^{2} + \|y\|_{A_{1}}^{2}} \\ &\leq 2 C_{0}(v) + 2 \inf_{y_{c} + \sum_{j=1}^{J} y_{j} = y}^{\int} \frac{\|y_{c}\|_{A}^{2} + \sum_{j=1}^{J} \|y_{j}\|_{A}^{2}}{\gamma |y|_{A_{0}}^{2} + \|y\|_{A_{1}}^{2}}. \end{split}$$

Notice that, since  $y_j \in V_j$ , we have  $y_j = P_j y_j = P_{1,j} y_j$ . We now introduce the following elementary inequality for  $t_1, t_2 > 0$  and  $s_1, s_2 > 0$ :

$$\frac{\gamma t_1 + s_1}{\gamma t_2 + s_2} = \frac{\gamma t_1}{\gamma t_2 + s_2} + \frac{s_1}{\gamma t_2 + s_2} \le \frac{t_1}{t_2} + \frac{s_1}{s_2}$$

With this in hand, it follows from Lemma 3.4 that

$$\begin{split} &\frac{\|y_c\|_A^2 + \sum_{j=1}^J \|y_j\|_A^2}{\gamma |y|_{A_0}^2 + \|y\|_{A_1}^2} \\ &= \frac{\|P_c y_c\|_A^2 + \sum_{j=1}^J \|P_j y_j\|_A^2}{\gamma |y|_{A_0}^2 + \|y\|_{A_1}^2} \\ &\leq \frac{\gamma \left(|P_{0,c} y_c|_{A_0}^2 + \sum_{j=1}^J |P_{0,j} y_j|_{A_0}^2\right) + \left(\|P_{1,c} y_c\|_{A_1}^2 + \sum_{j=1}^J \|P_{1,j} y_j\|_{A_1}^2\right)}{\gamma |y|_{A_0}^2 + \|y\|_{A_1}^2} \\ &\leq \frac{|P_{0,c} y_c|_{A_0}^2 + \sum_{j=1}^J |P_{0,j} y_j|_{A_0}^2}{|y|_{A_0}^2} + \frac{\|y_c\|_{A_1}^2 + \sum_{j=1}^J \|y_j\|_{A_1}^2}{\|y\|_{A_1}^2} \\ &\leq \frac{|y_c|_{A_0}^2 + \sum_{j=1}^J |y_j|_{A_0}^2}{|y|_{A_0}^2} + \frac{\|y_c\|_{A_1}^2 + \sum_{j=1}^J \|y_j\|_{A_1}^2}{\|y\|_{A_1}^2}. \end{split}$$

The upper bound in (3.15) is obtained by taking infimum over all decompositions of  $y \in \text{Ker}(A_0)^{\perp}$  on the right-hand side. To show the lower bound in (3.15), note that for any decomposition, we have

$$||v||_A^2 = ||v_c + \sum_{j=1}^J v_j||_A^2 \le 2||v_c||_A^2 + 2||\sum_{j=1}^J v_j||_A^2 \le 2||v_c||_A^2 + 2\sum_{j=1}^J ||v_j||_A^2.$$

Therefore, taking the infimum over all possible decompositions, we can obtain the lower bound and conclude the proof.

Now we have results on our preconditioning method's uniform condition number estimation. In the following two subsections, we show that the assumptions (3.9) and (3.10) are valid in the context of the algebraic systems that we are considering.

**3.3.** Kernel decomposition condition. We continue with defining the subspace splitting that will satisfy the kernel condition in (3.9). At the same time, we bear in mind to choose a decomposition that intuitively follows (3.10) as well.

Consider characterizing the kernel of the matrix  $A_0$  as

$$\operatorname{Ker}(A_{0}) = \{v = (v_{\Omega}, v_{\Gamma}) \in V : a_{0}(v, v) = m_{\Gamma}(Rv, Rv) = 0\}$$

$$= \{v = (v_{\Omega}, v_{\Gamma}) \in V : v_{\Gamma} = \sigma(v_{\Omega})\}$$

$$= \left\{\begin{pmatrix} I_{\Omega} \\ \sigma \end{pmatrix} v_{\Omega} : v_{\Omega} \in V_{\Omega} \right\}.$$
(3.16)

Therefore, we can fully represent  $\operatorname{Ker}(A_0)$  with the vectors from the subspace  $V_{\Omega}$ . We take this into account when constructing the subspaces  $V_j \subset V$ ,  $V_c + \sum_{j=1}^J V_j = V$ . Descriptively, we should find a partition of V so that each part contains at least one spanning vector of  $\operatorname{Ker}(A_0)$  with a minimal overlap between the subspaces. Note that we first start with the subspaces  $V_j$ ,  $j \geq 1$ , which define the Schwarz preconditioner S, and then we construct the coarse space  $V_c$  via vertex aggregation since we consider aggregation-based AMG.

For each graph vertex  $j \in \mathcal{V}_{\Omega}$ , define the neighborhood of j in terms of the sparsity pattern of the operator R, that is,

(3.17)

$$\mathcal{N}_j = \{i \in \mathcal{V}_{\Gamma} : \left(\sigma\left(e_j^{\Omega}\right)\right)_i \neq 0, \ e_j^{\Omega} \in V_{\Omega}\}, \quad \text{where } \left(e_j^{\Omega}\right)_k = \begin{cases} 1, & k = j, \\ 0, & k \neq j, \end{cases} \qquad j \in \mathcal{V}_{\Omega}.$$

Specifically, the neighborhoods  $\mathcal{N}_j$  are the subsets of all the vertices in  $\mathcal{V}_{\Gamma}$  that the vertex  $j \in \mathcal{V}_{\Omega}$  restricts to by the action of restriction operator  $\sigma$ . Note that  $\mathcal{N}_j = \emptyset$  if  $\sigma(e_j^{\Omega}) = 0$ , which means that vertex  $j \in \mathcal{V}_{\Omega}$  does not connect to any vertex in  $\mathcal{V}_{\Gamma}$  via operator  $\sigma$ . Since  $\sigma$  is surjective, we have that

(3.18) 
$$\bigcup_{j=1}^{N_{\Omega}} \mathcal{N}_{j} = \mathcal{V}_{\Gamma} \quad \text{and} \quad \bigcup_{j=1}^{N_{\Omega}} (\mathcal{N}_{j} \cup \{j\}) = \mathcal{V}_{\Gamma} \cup \mathcal{V}_{\Omega} = \mathcal{V}.$$

Hence, we have constructed a partition of the vertices of the graph in overlapping subsets, and we use this below to define the partition of unity needed in the analysis of the Schwarz smoother.

We now consider the subspaces  $V_i \subset V$  defined as

$$(3.19) V_j = \operatorname{span}\left(\left\{\begin{pmatrix} e_j^{\Omega} \\ 0 \end{pmatrix}\right\} \cup \left\{\begin{pmatrix} 0 \\ e_i^{\Gamma} \end{pmatrix}, i \in \mathcal{N}_j\right\}\right) \subset V, j \in \mathcal{V}_{\Omega},$$

with  $e_i^{\Gamma} \in V_{\Gamma}$  the unit vector in vertex  $i \in \mathcal{N}_j$ . Since  $\bigcup_{j=1}^{N_{\Omega}} (\mathcal{N}_j \cup \{j\}) = \mathcal{V}$ , it is straightforward to see that  $\sum_{j=1}^J V_j = V$ . It also follows that the number of subspaces is  $J \leq N_{\Omega} + 1$ , and if any  $\mathcal{N}_j = \emptyset$ , then  $V_j = \operatorname{span}\{\binom{e_j^{\Omega}}{0}\}$ . More precisely, that means that outside the domain of influence of the restriction operator  $\sigma$ , the subspaces are defined only on the support of the local finite element function of that DOF. In turn, that means that "around"  $\Gamma$ , we have an overlapping Schwarz method as the smoother, while in the rest of the domain, the subspaces define a standard pointwise smoother (Jacobi or Gauss-Seidel method).

Next, we define the coarse space  $V_c$  given by the UA-AMG method. Other constructions of coarse spaces are also possible, but we choose UA-AMG because the analysis in this case is more transparent and concise. The aggregates are constructed from the set of vertices  $\mathcal{V} = \{1, 2, \dots, N\}$  as follows:

(3.20a)

Splitting: 
$$\{1,\ldots,N\} = \bigcup_{k=1}^{n_{agg}} \mathfrak{a}_k$$
,  $\mathfrak{a}_l \cap \mathfrak{a}_k = \emptyset$ , when  $l \neq k$ ,  $|\mathfrak{a}_k| \leq C_{agg}$ ,  $k = 1,\ldots,n_{agg}$ , (3.20b)

Approximation: for 
$$v \in V$$
,  $v \approx v_c = \sum_{k=1}^{n_{agg}} v_{\mathfrak{a}_k}$ , where  $v_{\mathfrak{a}_k} = \frac{\langle \mathbb{1}_{\mathfrak{a}_k}, v \rangle_{\ell^2}}{|\mathfrak{a}_k|} \mathbb{1}_{\mathfrak{a}_k}$ ,

where  $\mathbb{1}_{\mathfrak{a}_k} \in \mathbb{R}^N$  is the indicator vector on every  $\mathfrak{a}_k$ ,  $|\mathfrak{a}_k|$  is the size of each aggregate,  $n_{agg}$  is the total number of aggregates (number of coarse grid DOFs), and  $C_{agg}$  is the maximal number of fine grid vertices in any aggregate.

Associated with the splitting of the vertices given in (3.18), we now introduce a partition of unity. Consider the following matrices, each associated with the support of the vector from the frame of  $Ker(A_0)$ :

(3.21) 
$$\chi_j = D_{\Omega}^{-1} \operatorname{diag}(\mathbb{1}_{\mathcal{N}_j \cup \{j\}}), \text{ where } D_{\Omega} = \sum_{j=1}^J \operatorname{diag}(\mathbb{1}_{\mathcal{N}_j \cup \{j\}}), \quad j = 1, \dots, J,$$

where  $\mathbb{1}_{\mathcal{N}_j \cup \{j\}}$  are the indicator vectors on a subset of vertices  $\mathcal{N}_j \cup \{j\} \subset \mathcal{V}$ . Clearly, the matrices  $\chi_j \in \mathbb{R}^{N \times N}$  and  $\sum_{j=1}^J \chi_j = I$ . The latter identity just means that  $\{\chi_j\}_{j=1}^J$  form a partition of unity. In addition, we have that  $\chi_j \chi_k = D_\Omega \chi_j (\chi_j \chi_k)$  and  $D_\Omega \chi_j (\chi_j - \chi_k) \chi_k$  is positive semidefinite.

Finally, the full subspace decomposition is given as follows: For  $v \in V$ ,

(3.22) 
$$v = v_c + \sum_{j=1}^{J} v_j$$
, where  $v_c = \sum_{k=1}^{n_{agg}} v_{\mathfrak{a}_k}$  and  $v_j = \chi_j(v - v_c)$ ,  $j = 1, \dots, J$ .

Based on the definitions of the kernel  $Ker(A_0)$  and the subspaces, we can verify that the space decomposition (3.19) satisfies the kernel decomposition condition (3.9), which is summarized in the following proposition.

PROPOSITION 3.6. Let  $V_j$ ,  $j=c,1,2,\ldots,J$ , be the subspaces of V defined in (3.19) and (3.20). Then  $\{V_c\} \cup \{V_j\}_{j=0}^J$  satisfy the kernel decomposition condition (3.9).

*Proof.* By definition, we have that  $\operatorname{Ker}(A_0) \cap V_c \subseteq \operatorname{Ker}(A_0)$  and  $\sum_{j=1}^J \operatorname{Ker}(A_0) \cap V_j \subseteq \operatorname{Ker}(A_0)$ . On the other hand, for any  $v \in \operatorname{Ker}(A_0)$ , we know that  $v = \begin{pmatrix} I_{\Omega} \\ \sigma \end{pmatrix} v_{\Omega}$  for some  $v_{\Omega} \in V_{\Omega}$ . Equivalently, the column vectors  $\{\mathbb{1}_{\mathcal{N}_j \cup \{j\}}\}_{j=1}^{N_{\Omega}}$  span  $\operatorname{Ker}(A_0)$ , which can be expanded as follows:

$$(3.23) \quad v = \sum_{j=1}^{N_{\Omega}} (v_{\Omega})_{j} \underbrace{\mathbb{1}_{\mathcal{N}_{j} \cup \{j\}}}_{\in \operatorname{Ker}(A_{0})}$$

$$= \sum_{j=1}^{N_{\Omega}} (v_{\Omega})_{j} \underbrace{\left[\begin{pmatrix} e_{j}^{\Omega} \\ 0 \end{pmatrix} + \sum_{i \in \mathcal{N}_{j}} \begin{pmatrix} 0 \\ e_{i}^{\Gamma} \end{pmatrix}\right]}_{\in \operatorname{V}_{j}} \in \sum_{j=1}^{N_{\Omega}} \operatorname{Ker}(A_{0}) \cap V_{j} \subseteq \sum_{j=1}^{J} \operatorname{Ker}(A_{0}) \cap V_{j}.$$

- **3.4. Stable decomposition condition.** Now that we have shown the kernel decomposition condition, we prove that the same subspace decomposition is also stable in both  $A_0$  and  $A_1$ -inner products.
- **3.4.1. Stability condition in A\_1.** We first focus on the positive definite operator  $A_1$  and the coarse space estimates, and we present the following immediate result on the stability estimates of the coarse space  $V_c$ .

LEMMA 3.7. For  $v \in V$  and its coarse grid approximation  $v_c = \sum_{k=1}^{n_{agg}} v_{\mathfrak{a}_k}$ , we have

$$(3.24) ||v - v_c||_{D_1}^2 \lesssim ||v||_{A_1}^2 \text{ and } ||v_c||_{A_1}^2 \lesssim ||v||_{A_1}^2,$$

with  $D_1$  being the diagonal of  $A_1$ .

*Proof.* The first estimate follows from Poincaré inequality (3.6) on each aggregate  $\mathfrak{a}_k$ ,  $k=1,\ldots,n_{aqq}$ , i.e.,

$$(3.25) \|v - v_c\|_{D_1}^2 = \sum_{k=1}^{n_{agg}} \|v - v_{\mathfrak{a}_k}\|_{D_1, \mathfrak{a}_k}^2 \lesssim \sum_{\mathfrak{a}_k} c_{\mathfrak{a}_k} \|v\|_{A_1, \mathfrak{a}_k}^2 \lesssim \left(\max_{\mathfrak{a}_k} c_{\mathfrak{a}_k}\right) \|v\|_{A_1}^2,$$

where  $c_{\mathfrak{a}_k}$  are the Poincaré constants on each aggregate  $\mathfrak{a}_k$ ; cf. [49], [61]. In addition,  $\|\cdot\|_{D_1,\mathfrak{a}_k}$  and  $\|\cdot\|_{A_1,\mathfrak{a}_k}$  denote the  $D_1$ - and  $A_1$ -norms restricted to the aggregate  $\mathfrak{a}_k$ , respectively.

The second estimate follows from the triangle inequality, (3.5), and (3.25), namely,

$$||v_c||_{A_1}^2 \lesssim ||v||_{A_1}^2 + ||v - v_c||_{A_1}^2 \lesssim ||v||_{A_1}^2 + ||v - v_c||_{D_1}^2 \lesssim ||v||_{A_1}^2.$$

Next, we consider estimates on the specific subspaces used for the Schwarz smoother (3.8b) (with using  $A_1$  instead of A), which is defined by taking the infimum over all possible decompositions of any fine scale function  $v \in V$  based on the space decomposition  $V = V_c + \sum_{j=1}^J V_j$ . We want to show the stability condition in the  $A_1$ -norm; that is, choosing the decomposition (3.22), we achieve a uniform bound on that infimum.

PROPOSITION 3.8. For any  $v \in V$ , let  $\{v_c\} \cup \{v_j\}_{j=1}^J$  be the subspace decomposition defined in (3.22). Then

(3.26) 
$$||v_c||_{A_1}^2 + \sum_{j=1}^J ||v_j||_{A_1}^2 \lesssim ||v||_{A_1}^2.$$

The stability constants hidden in " $\lesssim$ " depend on the maximal number of nonzeros per row in  $A_1$ ; the maximum of the local Poincaré constants of each aggregate  $\mathfrak{a}_k$ ,  $k = 1, \ldots, n_{agg}$ ; and the maximum over the number of intersections between the subspaces  $V_j$ ,  $j = 1, \ldots, J$ .

*Proof.* Using (3.5), the definition of  $\chi_j$ , and Lemma 3.7, we obtain that

$$\begin{split} \|v_c\|_{A_1}^2 + \sum_{j=1}^J \|v_j\|_{A_1}^2 &= \|v_c\|_{A_1}^2 + \sum_{j=1}^J \|\chi_j(v-v_c)\|_{A_1}^2 \\ &\lesssim \|v_c\|_{A_1}^2 + \sum_{j=1}^J \|\chi_j(v-v_c)\|_{D_1}^2 \qquad \text{(from (3.5))} \\ &\lesssim \|v_c\|_{A_1}^2 + \|v-v_c\|_{D_1}^2 \qquad \text{(by the definition of $\chi_j$)} \\ &\lesssim \|v\|_{A_1}^2 \qquad \qquad \text{(from Lemma 3.7).} \quad \Box \end{split}$$

**3.4.2. Stability condition in**  $A_0$ . Finally, to prove the stability of the decomposition in the  $A_0$ -seminorm, it is necessary to specify some properties of the lower-order term  $a_0(\cdot, \cdot)$ . While it slightly limits the applicability of our approach, the example problems we are considering in section 4 adhere to the required assumptions.

Let  $L: \mathcal{V}_{\Gamma} \to \mathcal{V}_{\Omega}$  be a metric function on the vertices of the graph such that

(3.27) 
$$L(i) = \arg\min\{\operatorname{dist}(i,j), j \in \mathcal{V}_{\Omega}\}, \quad i \in \mathcal{V}_{\Gamma}.$$

The metric  $\operatorname{dist}(\cdot,\cdot)$  can be any metric between the graph vertices in  $\mathcal{V}_{\Gamma}$  and  $\mathcal{V}_{\Omega}$ . For example, in the reduced EMI example, it can be  $\operatorname{dist}(i,j) := \|p_i - p_j\|$ , where  $p_i$  and  $p_j$  are the spatial locations of the vertex  $i \in \mathcal{V}_{\Gamma}$  and  $j \in \mathcal{V}_{\Omega}$ , respectively. The function  $L(\cdot)$  is single-valued, but its pseudoinverse is possibly set-valued and can be extended to the whole  $\mathcal{V}$ . More specifically, the inverse  $L^{-1}: \mathcal{V}_{\Omega} \to \mathcal{V}_{\Gamma}$  and its extension  $\tilde{L}: \mathcal{V}_{\Omega} \to \mathcal{V}$  are defined as

(3.28) 
$$L^{-1}(j) = \{i \in \mathcal{V}_{\Gamma} : L(i) = j\}, \quad \tilde{L}(j) = \{j\} \cup L^{-1}(j), \quad j \in \mathcal{V}_{\Omega}.$$

Note that if for  $j_1, j_2 \in \mathcal{V}_{\Omega}$ ,  $j_1 \neq j_2$ , then  $L^{-1}(j_1) \cap L^{-1}(j_2) = \emptyset$ , and consequently  $\tilde{L}(j_1) \cap \tilde{L}(j_2) = \emptyset$ . Also, it is possible to have  $L^{-1}(j) = \emptyset$ , and that holds for  $j \in \mathcal{V}_{\Omega}$ , which do not interpolate any  $i \in \mathcal{V}_{\Gamma}$ . For example, in the reduced EMI equations, that applies to the "interior" DOFs of the three-dimensional subdomain that have no contribution in the averaging operator  $\sigma$ . On the other hand, note that  $\tilde{L}(j) \neq \emptyset$  and is surjective for all  $j \in \mathcal{V}$ . This motivates us to redefine the lower-order term  $a_0(\cdot, \cdot)$  from (3.7c) to

(3.29) 
$$a_0(u,v) = \sum_{i \in \mathcal{V}_{\Gamma}} m_i (u_{\Gamma,i} - u_{L(i)}) (v_{\Gamma,i} - v_{L(i)}),$$

and the seminorm becomes

(3.30) 
$$|v|_{A_0}^2 = \sum_{j \in \mathcal{V}_{\Omega}} \sum_{i \in L^{-1}(j)} m_i (v_{\Gamma,i} - v_{\Omega,j})^2, \qquad v = (v_{\Omega}, v_{\Gamma}) \in V.$$

In this setting, we can easily represent the kernel of the matrix  $A_0$ , that is,

(3.31) 
$$\operatorname{Ker}(A_0) = \operatorname{span}\{\mathbb{1}_{\tilde{L}(j)}, j \in \mathcal{V}_{\Omega}\};$$

thus, the size of  $\operatorname{Ker}(A_0)$  can be as large as the number of vertices in  $\mathcal{V}_{\Omega}$ . Notice, however, that  $\operatorname{Ker}(A_0)$  is not equal to  $V_{\Omega}$ , as it also involves the coupling between elements of  $V_{\Gamma}$  and  $V_{\Omega}$ . By definition, the aggregates  $\mathfrak{a}_k$ ,  $k = 1, \ldots, n_{agg}$ , are disjoint subsets of  $\mathcal{V}$ , and hence for every  $i \in \mathcal{V}$ , there exists a unique  $k \in \{1, \ldots, n_{agg}\}$  such

that  $i \in \mathfrak{a}_k$ , and we denote  $\mathfrak{a}(i) := \mathfrak{a}_k$ . In accordance with this, we make an assumption that the aggregates are constructed as follows:

(3.32) 
$$\mathfrak{a}(j) = \tilde{L}(j), \quad j \in \mathcal{V}_{\Omega} \quad \text{such that} \quad L^{-1}(j) \neq \emptyset.$$

Such an assumption is not restricting our approach, as the sets  $L^{-1}(j)$  are well-defined, and for  $j_1 \neq j_2$ , where  $j_1, j_2 \in V_{\Omega}$ , these sets are disjoint. The aggregation can be constructed by first choosing  $\tilde{L}(j)$  as aggregates as long as  $L^{-1}(j) \neq \emptyset$ . In such a case, for a given  $v \in V$  and  $v_c = \sum_{k=1}^{n_{agg}} v_{\mathfrak{a}_k} \in V_c$ , we have that  $a_0(v_c, v_c) = 0$ ; that is, the form  $a_0(\cdot, \cdot)$  vanishes on the coarse space. As a consequence, we have the stability of the decomposition (3.22) in  $A_0$ .

PROPOSITION 3.9. For any  $v \in V$ , let  $\{v_c\} \cup \{v_j\}_{j=1}^J$  be the subspace decomposition defined in (3.22). Then

$$(3.33) |v_c|_{A_0}^2 + \sum_{j=1}^J |v_j|_{A_0}^2 \lesssim |v|_{A_0}^2;$$

that is, the decomposition is stable in the  $A_0$ -seminorm. The stability constants depend on the maximal number of nonzeros per row in  $A_0$ ; the maximum of Poincaré constants of each aggregate  $\mathfrak{a}_k$ ,  $k = 1, \ldots, n_{agg}$ ; and the maximum the number of nontrivial intersections between the subspaces  $V_j$ ,  $j = 1, \ldots, J$ .

*Proof.* The proof follows analogously to the proof of Proposition 3.8 by replacing  $A_1$  with  $A_0$  and  $D_1$  with the diagonal of  $A_0$  and noting that  $|v_c|_{A_0} = 0$  for the coarse space functions  $v_c = \sum_{k=1}^{n_{agg}} v_{\mathfrak{a}_k} \in V_c$ .

3.5. On the multiplicative version of the preconditioner. As is well known [59, 20], additive and multiplicative versions of a two-level AMG preconditioner, including the preconditioner described in this paper, are closely related. Starting with the smoother, the multiplicative smoother  $S_{mult}$  is defined as  $I - S_{mult}A := \prod_{j=1}^{J} (I - P_j)$  and, based on the well-known result in many references (see, e.g., [59], [20], [57], [63, Lemma 3.3]), is equivalent to the additive smoother S in (3.8). In particular, the following inequality holds for  $w \in V$ :

(3.34) 
$$\frac{1}{4} \|w\|_{S^{-1}}^2 \lesssim \|w\|_{S_{mult}}^2 \lesssim \|w\|_{S^{-1}}^2.$$

The upper bound only depends on the maximal degree in the graph of subspaces  $\{V_j\}_{j=1}^J$  with vertices  $\{1,\ldots,J\}$  and edges given by pairs of indices (i,j) for which  $V_j \cap V_i \neq \{0\}$ . That is the maximal number of intersections of any subspace  $V_j$  with other subspaces  $V_i$ ,  $i \neq j$ . Similarly, we define the multiplicative version of the two-level AMG preconditioner  $B_{mult}$  as  $I - B_{mult}A := (I - P_cA)(I - S_{mult}A)$ . An inequality in the same form of (3.34) with S and  $S_{mult}$  replaced by B and  $B_{mult}$ , respectively, can be established based on the same arguments. Such an inequality shows the equivalence between B and  $B_{mult}$ . The theoretical estimate regarding the convergence of  $B_{mult}$  is basically similar to the result of [36, Theorem 4.2] and thus is omitted here. We comment that such a result is an analogue of the condition number estimate of B given in Theorem 3.5.

Using the techniques which we have employed in showing stability for the subspace decomposition in the  $A_1$ -norm, we can show the "weak" approximation property, which is a necessary and sufficient condition for uniform two-level AMG convergence [26], [63, Theorem 3.5]. The approximation result reads as follows: For any  $v \in V$ ,

there exists  $v_c \in V_c$  such that the following estimates hold independently of parameters h and  $\gamma$ :

(3.35) 
$$||v - v_c||_{S_{mult}}^2 \lesssim ||v||_{A_\iota}^2, \quad \iota \in \{0, 1\},$$

where we can take  $v \in \text{Ker}(A_0)^{\perp_{A_1}}$  for  $\iota = 0$ . This estimate, which follows from the results we have shown for the additive preconditioner, gives the uniform convergence of the multiplicative method.

- 4. Implementation. We dedicate this section to explaining what the convergence conditions mean and how they can be utilized to construct uniformly convergent multilevel methods in different applications, namely, with regard to example problems in section 2. Moreover, we confirm the theory with numerical results<sup>1</sup> that are obtained using software components HAZniCS [8]. Unless stated otherwise, the finite element problems are assembled using FEniCS [40] and FEniCS<sub>ii</sub> [31].
- **4.1. Bidomain model.** Consider A and M to be the matrix representations of the Laplacian  $-\Delta: V \to V'$  and the  $L^2$ -inner product on V, respectively. With  $\bar{V} = V \times V$ , let  $\bar{K} = (\bar{A} + \gamma \bar{M}): \bar{V} \to \bar{V}'$  represent the system operator in (2.2), where

$$\bar{A} = \begin{pmatrix} \alpha_e A & \\ & \alpha_i A \end{pmatrix}$$
 and  $\bar{M} = \begin{pmatrix} M & -M \\ -M & M \end{pmatrix}$ .

Furthermore, denote a coarse space  $V_c \subset V$  and the corresponding (surjective) prolongation operator  $P: V_c \to V$ , and combine  $\bar{V}_c = V_c \times V_c$  and  $\bar{P}: \bar{V}_c \to \bar{V}$ . As mentioned in subsection 3.5, the necessary and sufficient condition for convergence of the two-level AMG method for solving (2.2) is the weak approximation property. If  $\bar{S}: \bar{V}' \to \bar{V}$  is the smoother for the two-level AMG method on  $\bar{K}$ , then we want that for any  $y \in \bar{V}$ , there exists  $y_0 \in \bar{V}_c$  such that

for some C>0. This is satisfied for standard (pointwise) smoothers such as the Jacobi or the Gauss–Seidel method, but they do not guarantee that the bound is independent of  $\gamma$ . On the other hand, following the theory derived in section 3, we can show that the smoother

(4.2) 
$$\bar{S}^{-1} = \begin{pmatrix} \alpha_e D_A + \gamma D_M & -\gamma D_M \\ -\gamma D_M & \alpha_i D_A + \gamma D_M \end{pmatrix}$$

satisfies the stability and kernel conditions, with  $D_M$  and  $D_A$  being diagonals of matrices M and A, respectively. Actually, we can directly prove the weak approximation property in this case by relying on two results from (3.5): For  $v \in V$ , there exists  $v_c \in V_c$  such that

$$(4.3) ||v - Pv_c||_{D_A}^2 \le C_A ||v||_A^2 \quad \text{and} \quad ||v - Pv_c||_{D_M}^2 \le C_M ||v||_M^2,$$

with  $C_A, C_M > 0$  depending only on the number of nonzeros per row in A and M, respectively. Take  $y = \begin{pmatrix} v_e \\ v_i \end{pmatrix} \in \bar{V}$ . Define  $w^+ = \frac{1}{2}(v_e + v_i)$  and  $w^- = \frac{1}{2}(v_e - v_i)$  so that

$$(4.4) y = \begin{pmatrix} w^- \\ -w^- \end{pmatrix} + \underbrace{\begin{pmatrix} w^+ \\ w^+ \end{pmatrix}}_{\in \text{Ker}(\bar{M})}.$$

 $<sup>^1{\</sup>rm Source}$  codes for all the examples are available at https://github.com/anabudisa/metric-amgexamples.

We know that  $w^+, w^- \in V$ , so there exist  $w_c^+, w_c^- \in V_c$  that satisfy (4.3). Taking  $y_c \in \bar{V}_c$  as  $y_c = {w_c^- \choose -w_c^-} + {w_c^+ \choose w_c^+}$ , it follows that

$$\begin{split} \|y - \bar{P}y_c\|_{\bar{S}^{-1}}^2 &= \| \begin{pmatrix} w^- - Pw_c^- \\ -(w^- - Pw_c^-) \end{pmatrix} \|_{\bar{S}^{-1}}^2 + \| \begin{pmatrix} w^+ - Pw_c^+ \\ w^+ - Pw_c^+ \end{pmatrix} \|_{\bar{S}^{-1}}^2 \\ &= (\alpha_e + \alpha_i) \left( \|w^- - Pw_c^-\|_{D_A}^2 + \|w^+ - Pw_c^+\|_{D_A}^2 \right) + 2\gamma \|w^- - Pw_c^-\|_{D_M}^2 \\ &\leq \max\{C_A, C_M\} \left( (\alpha_e + \alpha_i) \left( \|w^-\|_A^2 + \|w^+\|_A^2 \right) + 2\gamma \|w^-\|_M^2 \right) \\ &= \max\{C_A, C_M\} \|y\|_{\bar{K}}^2. \end{split}$$

It is possible to notice where a pointwise smoother would fail to control (with regard to  $\gamma$ ) functions  $y \in V$ , where the kernel part in (4.4) is nonzero. For example, for a Jacobi smoother given as the diagonal of the system matrix  $\bar{K}$  (which only contains  $D_A$ ), we are left with an extra term  $2\gamma ||w^-||_M^2$  in the third line in the above proof which is unbounded in  $\gamma$ .

Interestingly, the UA-AMG method for  $\bar{K}$  handles the near-kernel functions naturally. Due to the two-by-two block structure of  $\bar{M}$  and the fact that M is a mass matrix, we can obtain a special prolongation operator:

$$\bar{P} = \begin{pmatrix} I_V \\ I_V \end{pmatrix} : \bar{V}_c \to \bar{V} \text{ and } \bar{V}_c = V.$$

That is, in the two-level method, each coarse space DOF is constructed by combining two fine scale DOFs that are coupled with  $\bar{M}$ , and the total number of DOFs in the coarse space is half of the fine scale space. Note that Range( $\bar{P}$ ) is exactly the near kernel of  $\bar{K}$ , which implies that the coarse grid correction will handle this type of function and simultaneously preserve stability.

This kind of construction is possible since the coupling is present in the whole domain and the DOFs in each subdomain align with each other. The more interesting case of lower-dimensional interface coupling is given in the following subsections, where both a special prolongation and a Schwarz smoother are needed for uniform convergence, even though the aim of this example is to show in a simple context what the conditions derived in subsection 3.2 mean and how uniform convergence can be obtained in any multilevel setting. Indeed, on grids obtained by a successful refinement, the UA-AMG discussed in this section resolves completely the near-kernel components of the error on the first coarse grid and, as a consequence, allows for the use of geometric multigrid hierarchies on coarser levels.

This is also numerically confirmed in the following results. First, we consider the problem (2.2) on a shape regular triangulation of a unit square domain  $\Omega = (0,1)^2$  and discretized with the continuous linear finite elements  $\mathbb{P}_1$ . To solve the problem, we use a conjugate gradient (CG) method preconditioned with different configurations of the AMG method, and we test the solver performance against mesh refinement and coupling strength. The common settings in all configurations are a two-level aggregation-based AMG method, one W-cycle per iteration, and a direct solver (UMFPACK [14]) on the coarse grid. We compare the performance of the UA-AMG and SA-AMG with or without the special prolongation (4.5) and with the kernel-aware Schwarz smoother (3.8b) or a pointwise (Gauss-Seidel) smoother. Both smoothers are applied in a symmetric multiplicative way.

The results are given in Figure 1. As expected, the regular AMG method (AMG in Figure 1) is fairly stable with regard to mesh refinement, but using a smoother that does not satisfy kernel conditions (3.9), we obtain a significant increase in the

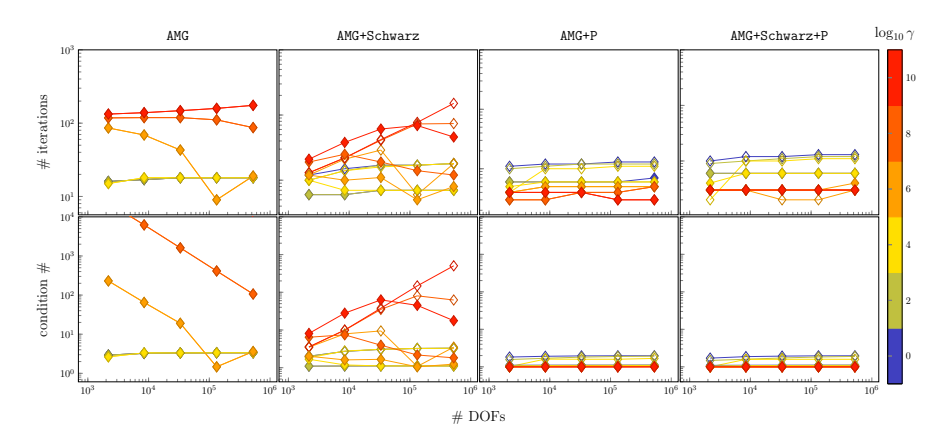


FIG. 1. Number of iterations and estimated condition number of the CG method preconditioned with aggregation-based AMG to solve the bidomain problem (2.2) in  $\Omega=(0,1)^2$ . We show the performance of the AMG preconditioner without regular prolongation and pointwise smoother operators, with using the Schwarz smoother (3.8b) satisfying the kernel conditions, with special prolongation in (4.5), and with using both the Schwarz smoother and special prolongation, which are, respectively, shown in the first, second, third, and fourth columns. Hollow marks indicate using the UA-AMG method and full marks using the SA-AMG method. The color of the lines indicates the magnitude of the coupling parameter  $\gamma$  ranging from 1 (blue) to  $10^{10}$  (red).

number of iterations and condition number with increasing  $\gamma$ . Replacing Gauss—Seidel with a kernel-aware Schwarz smoother (4.2) (AMG+Schwarz), we see a more robust performance with regard to the coupling parameters  $\gamma$ . However, the Schwarz smoother may influence the stability conditions (3.33), resulting in the increase of number of iterations for finer meshes in the case of UA-AMG. This behavior is stabilized using the prolongation operator (4.5) (AMG+P with only prolongation (4.5) and AMG+Schwarz+P with both smoother (4.2) and prolongation (4.5)), which confirms the theory that both kernel and stability conditions are necessary for the uniform convergence. Moreover, the AMG preconditioner with the prolongation operator  $\bar{P}$  performs similarly when using the kernel-aware smoother  $\bar{S}$  or not. As mentioned, Range( $\bar{P}$ ) is exactly the near kernel of  $\bar{K}$ , so both convergence conditions are already satisfied. Thus, in this specific example, it is most efficient to use the method AMG+P. If Range( $\bar{P}$ ) did not contain the near kernel of the system operator, we would need to use the method with an additional kernel-aware Schwarz smoother (AMG+Schwarz+P) to retain uniform convergence.

Additional performance results of the AMG-preconditioned CG method are shown in a three-dimensional setting in Figure 2. We consider again a shape regular simplicial mesh of the unit cube domain  $\Omega=(0,1)^3$  and  $\mathbb{P}_1$  finite element discretization. We study the number of CG iterations, condition number, and CPU time consumption with regard to mesh refinement and coupling parameter magnitude. The computations for this example are performed on a workstation with a 3.9 GHz Intel Core i7-1065G7 CPU and 32 GB of RAM. We can conclude that while the AMG preconditioner, both with and without using the prolongation operator (4.5), performs uniformly with regard to the system size, the prolongation operator is definitely needed to achieve stable performance for larger values of  $\gamma$ .

Remark 4.1 (geometric multrigrid). The bidomain smoother (4.2) can be viewed as a Schwarz smoother for DOFs located at a "star"-patch/macroelement of each vertex. To show robustness of our approach in the geometric multigrid setting, we

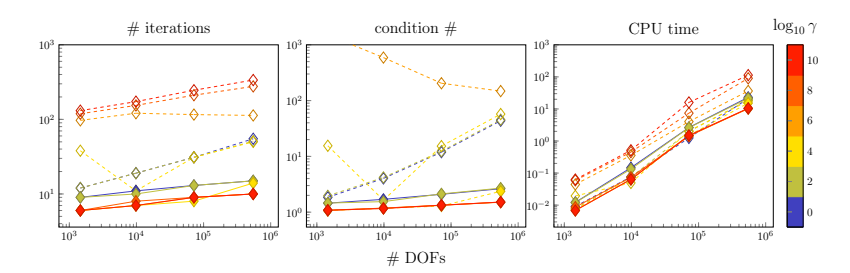


Fig. 2. Number of iterations, estimated condition number, and total solving CPU time of the CG method preconditioned with UA-AMG to solve the bidomain problem (2.2) in  $\Omega = (0,1)^3$ , shown in the first, second, and third columns, respectively. We compare the performance of the standard AMG preconditioner (marked with dashed lines) and AMG with using the special prolongation in (4.5) (marked with full lines). The color of the lines indicates the magnitude of the coupling parameter  $\gamma$  ranging from 1 (blue) to  $10^{10}$  (red).

Table 1 Number of preconditioned CG iterations using a geometric multigrid and smoother (2.1) for bidomain equation (2.2) with  $\Omega = (0,1)^2$  and discretization by  $\mathbb{P}_1$ -elements.

#DOFs $\gamma$	1	$10^{2}$	$10^{4}$	$10^{6}$	$10^{8}$	$10^{10}$
2178	19	19	18	19	19	20
8450	19	19	18	18	19	19
33282	19	19	17	17	19	19
132098	19	19	17	17	17	18
526338	19	19	17	17	17	17

implemented a multigrid preconditioner for (2.2) using the PCPATCH framework [16] for the required space decompositions. The finite element discretization was done with the Firedrake [47] library, which provides a convenient interface to PCPATCH preconditioners. Using the two-dimensional geometry from subsection 4.1, we show in Table 1 the number of CG iterations required for convergence with relative error tolerance of  $10^{-10}$ . The preconditioner applied a single V-cycle per CG iteration. We observe that the iteration counts are bounded in mesh size and the coupling parameter  $\gamma$ .

**4.2. EMI model.** We next investigate the performance of the proposed AMG method for solving the EMI model (2.3) in both two-dimensional and three-dimensional settings. In the former case, we let  $\Omega_i = (0,1) \times (0,\frac{1}{2})$ ,  $\Omega_e = (0,1) \times (\frac{1}{2},1)$ , while in three dimensions,  $\Omega_i = (0,1)^2 \times (0,\frac{1}{2})$ ,  $\Omega_e = (0,1)^2 \times (\frac{1}{2},1)$ . In both cases, Dirichlet conditions are prescribed on boundary surfaces parallel with the interface  $\Gamma$ . Neumann conditions are set on the remaining parts of the boundary. The systems (2.4) are then discretized by  $\mathbb{P}_1$  elements and solved by the preconditioned CG method. Following subsection 4.1, the preconditioner uses UA-AMG with a maximum of 10 levels and a Schwarz smoother (3.8b). With this setup, the number of iterations required for reducing the initial preconditioned residual norm by  $10^{10}$  is given in Table 2. In both two-dimensional and three-dimensional cases, the iterations are bounded in the coupling strength.

4.3. Reduced one-dimensional EMI model. In the case of mixed-dimensional modeling, the interface coupling is usually supported on and in a close neighborhood of the lower-dimensional subdomain, where the higher-dimensional quantity is projected using a trace or an averaging operator  $\Pi_{\rho}$ . Hence, the representation of the

Table 2
Number of preconditioned CG iterations required for solving the EMI model (2.3) with AMG using smoother (3.8b).

$\Omega_i \cup \Omega_e = (0,1)^2$						$\Omega_i \cup \Omega_e = (0,1)^3$							
#DOFs	1	$10^{2}$	$10^{4}$	$10^{6}$	$10^{8}$	$10^{10}$	#DOFs	1	$10^{2}$	$10^{4}$	$10^{6}$	$10^{8}$	$10^{10}$
4290	16	15	15	15	15	15	150	3	3	3	3	3	3
16770	18	18	18	18	18	18	810	5	6	6	6	6	6
66306	19	19	19	19	19	19	5202	8	9	9	9	9	9
263682	20	21	20	20	20	20	37026	13	13	13	13	13	13
1051650	21	22	20	20	20	20	278850	17	17	16	16	16	16

kernel of the coupling term is tightly linked to the representation of the operator  $\Pi_{\rho}$ . In the following, we show how the choice of the operator  $\Pi_{\rho}$  influences the choice of Schwarz subspaces and how the algebraic kernel and stability conditions induce a geometric multigrid method to solve the three-dimensional/one-dimensional coupled problem (2.5).

Assume that we are given simplicial meshes of  $\Omega$  and  $\Gamma$ , i.e.,  $\mathcal{T}_h^{\Gamma}$  and  $\mathcal{T}_h^{\Omega}$ , which do not necessarily match. Additionally, assume that  $V = V_{\Omega} \times V_{\Gamma}$  is a nodal-based FEM approximation, e.g.,  $V_{\Omega} = \mathbb{P}_1(\Omega)$  and  $V_{\Gamma} = \mathbb{P}_1(\Gamma)$ . We can define the interface (metric) operator similarly to (3.2) as  $R = (-\Pi_{\rho} I_{\Gamma})$ . Denote also  $n_{\Omega} = \dim V_{\Omega}$ ,  $n_{\Gamma} = \dim V_{\Gamma}$ , and  $n = \dim V = n_{\Omega} + n_{\Gamma}$ . Then we describe the kernel of coupling operator  $A_0 = R^T M_{\Gamma} R$  as

$$(4.6) \qquad \operatorname{Ker}(A_0) = \left\{ \begin{pmatrix} v_{\Omega} \\ v_{\Gamma} \end{pmatrix} \in V : \Pi_{\rho} v_{\Omega} = v_{\Gamma} \right\} = \left\{ \begin{pmatrix} v_{\Omega} \\ \Pi_{\rho} v_{\Omega} \end{pmatrix}, v_{\Omega} \in V_{\Omega} \right\}.$$

We can decompose the whole space as  $V = \text{Ker}(A_0) \oplus \text{Ker}(A_0)^{\perp}$ , where  $\perp$  regards the orthogonality in the A-norm, with  $A = A_1 + \gamma A_0$  and  $A_1 = \text{diag}\{A_{\Omega}, A_{\Gamma}\}$ . We closely follow the derivation in subsection 3.3 to find a Schwarz decomposition of V that satisfies the kernel condition (3.9).

Assume some ordering of DOFs in  $V_{\Omega}$  and  $V_{\Gamma}$ . Motivated by the kernel characterization in (4.6), we can say that for every  $i \in \{1, ..., n_{\Omega}\}$ , we define

$$\mathcal{N}_{\Gamma}(i) = \{k \in \{1, \dots, n_{\Gamma}\} : (R)_{ki} \neq 0\},\$$

where  $(R)_{ij}$  is the element in R in ith row and jth column. Therefore, for each  $i \in \{1, \ldots, n_{\Omega}\}$ , we define

(4.8) 
$$\mathcal{T}_h^i = \{ \tau \in \mathcal{T}_h^{\Omega} : \boldsymbol{x}^i \in \tau \} \cup \{ \tau \in \mathcal{T}_h^{\Gamma} : \boldsymbol{x}^k \in \tau, \, k \in \mathcal{N}_{\Gamma}(i) \},$$

(4.9) 
$$\Omega_h^i = \operatorname{int}\left(\bigcup \mathcal{T}_h^i\right),$$

where  $x^{j}$  are the coordinates of the node j. Then the Schwarz subspaces are given by

$$(4.10) \quad V_i = \left\{ v = \begin{pmatrix} v_{\Omega} \\ v_{\Gamma} \end{pmatrix} \in V : \operatorname{supp}(v) \subset \bar{\Omega}_h^i \right\}, \quad i \in \{1, \dots, n_{\Omega}\}, \quad \text{ and } \quad V = \sum_{i=1}^{n_{\Omega}} V_i.$$

Using this definition and with simple computation, it follows that  $\operatorname{Ker}(A_0) = \sum_{i=1}^{n_{\Omega}} \operatorname{Ker}(A_0) \cap V_i$ .

This construction of Schwarz subspaces is used in the following numerical example. The problem is defined by the geometry illustrated in the right part of Figure 3. The neuron geometry is obtained from the NeuroMorpho.Org inventory of digitally reconstructed neurons and glia [41]. The neuron from a mouse's brain

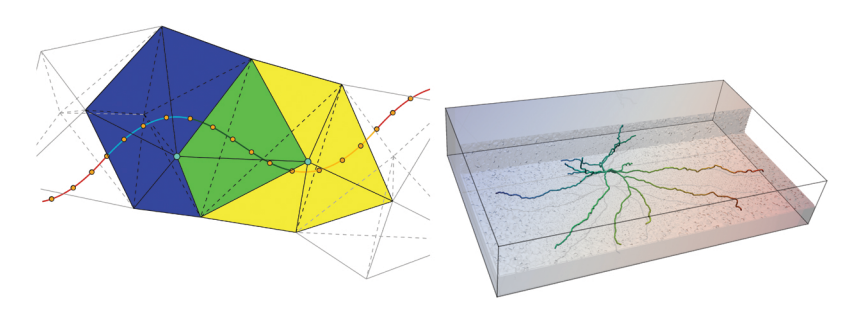


Fig. 3. (Left) Illustration of overlapping Schwarz subspaces for an example of nonfitted mesh for the coupled three-dimensional/one-dimensional problem (2.5). Assuming nodal finite element discretization, each Schwarz subspace (in blue and yellow) is local and contains the support of functions (three dimensions and one dimension) defined in DOFs that are coupled via the operator  $\Pi_{\rho}$ . Here, the radius of coupling  $\rho$  contains only the closest three-dimensional nodes (in light blue). The overlap is marked in green. (Right) Domain geometry of the three-dimensional/one-dimensional problem (2.5) The one-dimensional domain is the neuron and the network of neuronal dendrites, while the three-dimensional domain (a shallow clip) represents extracellular space. The outline of the three-dimensional domain is marked with black lines.

includes only dendrites (no axon or soma) and a total of 25 branches. It is embedded in a rectangular box of approximate dimensions of 222  $\mu$ m × 369  $\mu$ m × 65  $\mu$ m. Then the mixed-dimensional geometry is discretized with an unstructured tetrahedron mesh fitted to  $\Gamma$ ; i.e., line segments in the mesh of  $\Gamma$  are also edges of the three-dimensional mesh of  $\Omega$ . We use  $\mathbb{P}_1$  finite elements for discretization of both the three-dimensional and the one-dimensional function spaces. In total, we have 3391127 DOFs for the three-dimensional problem and 7281 DOFs for the one-dimensional problem. Additionally, we enforce homogeneous Neumann conditions on the outer boundary of both subdomains.

To obtain the numerical solution, we use the CG method preconditioned with the AMG method described in section 3. The convergence is considered reached if the  $l_2$  relative residual norm is less than  $10^{-6}$ . We choose the SA-AMG that uses the block Schwarz smoother (symmetric multiplicative) defined by the kernel decomposition (4.10) for the DOFs that couple with regard to  $\Pi_{\rho}$  and the symmetrized Gauss–Seidel smoother on the three-dimensional interior DOFs. We study the performance of our solver with regard to parameters  $\gamma$  that, resulting from the coupled membrane ODE from the full EMI model, relates to the inverse of the time step size  $\Delta t$ , the coupling/dendrite radius  $\rho$ , and the membrane capacitance  $C_m$  [7]. That said, the intra- and extracellular conductivities and membrane capacitance parameters remain constant and fixed throughout their respective domains to  $\alpha_e = 3 \text{ mS cm}^{-1}$ ,  $\alpha_i = 7 \text{ mS cm}^{-1}$ , and  $C_m = 1 \mu\text{F cm}^{-2}$  [6], while we vary the time step size and coupling radius.

The results given in Table 3. The first three rows use the averaging operator (2.6) as the coupling operator between three-dimensional and one-dimensional DOFs with the radius  $\rho$  as the coupling radius. Thus, the Schwarz subspaces (4.10) are larger with larger  $\rho$ , and evaluating the Schwarz smoother may become expensive. On the other hand, using a weighted average and defining the value of the one-dimensional DOF by averaging of the values of the three-dimensional DOFs at the same element (at a distance at most h from the one-dimensional DOF) results in Schwarz subspaces of a smaller dimension. Hence, even though the number of iterations is slightly larger, the application of the Schwarz smoother in this case is computationally cheaper than

Table 3

Number of preconditioned CG iterations required for solving the reduced EMI model (2.5) with AMG using smoother (3.8b). (\*) denotes that we are using the three-dimensional-to-one-dimensional trace operator as the coupling operator.

$\rho \ [\mu \mathrm{m}] \qquad (\Delta t)^{-1} \ [\mathrm{s}^{-1}]$	1	$10^{2}$	$10^{4}$	$10^{6}$	$10^{8}$	$10^{10}$
5.0	2	2	2	3	3	4
1.0	2	2	2	3	3	4
0.2	2	2	2	3	4	4
0.0*	5	5	6	8	10	10

the case when the averaging is done using the prescribed physical radius. Note that we still need to scale the physical parameters for intracellular space and membrane due to dimension reduction, and we use  $\rho=1~\mu\mathrm{m}$ . Additionally, we note that this type of averaging corresponds to an implementation of the three-dimensional-to-one-dimensional trace operator, but such problem formulation is not well-posed in standard norms and can cause issues with h-refinement [18]. In summation, we observe a stable number of CG iterations in all cases considered; that is, the method is robust with regard to the problem parameters.

5. Conclusions. We have developed an AMG method to solve coupled interface-driven multiphysics problems. The method is aggregation based and introduces a custom Schwarz smoother that specifically handles the strongly weighted lower-order term on the interface. We state two conditions, the kernel and the stability conditions, required for the Schwarz decomposition and the aggregation to ensure uniform convergence of the two-level method. The conditions are constructive, and the method is purely algebraic, only requiring information on the coupling of the interface DOFs. This means that the solver can be easily implemented and applied to a variety of PDE systems. Additionally, the solver can also be realized in a geometric multigrid way, allowing for direct grid refinement around lower-dimensional inclusions. We have highlighted the effectiveness of the proposed solver to solve problems arising in models of electrical activity of excitable cells, specifically the bidomain equations, the EMI equations, and the three-dimensional/one-dimensional coupled EMI equations.

Appendix A. Finite element matrices and graph Laplacians. We now show that a finite element discretization of an elliptic PDE is spectrally equivalent to a weighted graph Laplacian problem. The constants of the spectral equivalence depend on the polynomial degree used for the discretization.

LEMMA A.1. Let  $\mathcal{T}_h$  be a simplicial mesh in  $\mathbb{R}^d$  and  $A_h \in \mathbb{R}^{N \times N}$  be the stiffness matrix corresponding to the discretization of an elliptic operator  $Lu := -\operatorname{div}(\kappa \nabla u)$  with piecewise polynomial space of N DOFs. Then  $A_h$  is spectrally equivalent to a weighted graph Laplacian,

$$(A.1) \langle A_h v, v \rangle_{\ell^2} = \langle A v, v \rangle_{\ell^2}, \langle A v, w \rangle_{\ell^2} := \sum_e \omega_e \delta_e v \, \delta_e w, v, w \in \mathbb{R}^N,$$

where, for DOFs  $i, j \in \{1, 2, ..., N\}$  and graph edge e = (i, j),  $\delta_e v = v_i - v_j$  are edge differences and  $\omega_e = \omega_{ij} > 0$ , j < i are edge weights.

*Proof.* Let us consider a simplex  $T \in \mathcal{T}_h$ . Let  $n_T$  be the number of DOFs in T, and define

$$(A.2) |v|_{1,\kappa}^2 := \int_T \kappa \nabla v \cdot \nabla v = |T| \int_{\widehat{T}} \widehat{\kappa} \left[ \Phi_T^{-1} \widehat{\nabla} \widehat{v} \right] \cdot \left[ \Phi_T^{-1} \widehat{\nabla} \widehat{v} \right],$$

$$|v|_A^2 := |T| \sum_{e \in \mathcal{E}_T} |e|^{-2} \omega_e (\delta_e v)^2, \quad \omega_e > 0, \ e \in \mathcal{E}_T,$$

where  $\mathcal{E}_T \subset \{1, \dots, n_T\} \times \{1, \dots, n_T\}$ , |e| is the length of the edge e, and  $\omega_e$  are to be specified soon. On a shape regular mesh, this can be taken to be the diameter of T. The only requirement on  $\mathcal{E}_T$  is that these edges (pairs of DOFs) contain all DOFs and that the corresponding graph with vertices  $\{1, \dots, n_T\}$  and edges  $\mathcal{E}_T$  is connected. The  $\hat{}$  denotes the standard mapping to the reference simplex in  $\mathbb{R}^d$ :

(A.3) 
$$\widehat{x} \in \widehat{T} \mapsto \Phi_T \widehat{x} + x_0 \in T, \quad \Phi_T = (x_1 - x_0, \dots, x_d - x_0).$$

Notice that  $\|\Phi_T^{-1}\| \approx |e|^{-1}$ , with equivalence constants depending on the shape regularity of the mesh. Then, for any choice of  $\omega_e > 0$ , we have that  $|v|_A$  is a norm on  $\mathbb{R}^N/\mathbb{R}$ , and, similarly,  $|v|_{1,\kappa}$  is also a norm on the same finite-dimensional space. These norms are equivalent, with constants of equivalence depending on the shape regularity of the mesh and the variations in  $\kappa$  in each element [61, Lemma 14.1]. The weights  $\omega_e$  can be chosen so as to minimize the constants in the spectral equivalence. Choosing  $\omega_e = \frac{1}{T} \int_T \kappa$  for all  $e \in \mathcal{E}_T$  works in all cases when  $\kappa$  is piecewise smooth. The proof is then concluded as follows (with  $v \in \mathbb{R}^N$ ):

$$(A.4) \qquad \langle A_h v, v \rangle_{\ell^2} = \sum_T |v|_{1,\kappa}^2 \approx \sum_T |T| \sum_{e \in \mathcal{E}_T} |e|^{-2} \omega_e (\delta_e v)^2 \approx |v|_A^2.$$

An instructive example of the spectral equivalence from Lemma A.1 is to consider the piecewise linear continuous elements on a shape regular mesh. Then we can choose A as follows:

(A.5) 
$$\langle Av, v \rangle = \sum_{e \in \mathcal{E}} |e|^{d-2} \omega_e (\delta_e v)^2, \quad \omega_e = \sum_{T \supset e} \frac{1}{T} \int_T \kappa.$$

With such choice, the constants in Lemma A.1 only depend on the shape regularity of the mesh.

Reproducibility of computational results. This paper has been awarded the "SIAM Reproducibility Badge: Code and data available" as a recognition that the authors have followed reproducibility principles valued by SISC and the scientific computing community. Code and data that allow readers to reproduce the results in this paper are available at https://github.com/anabudisa/metric-amg-examples and in the supplementary materials (metric-amg-examples-master.zip [local/web 30KB]).

## REFERENCES

- A. AGUDELO-TORO AND A. NEEF, Computationally efficient simulation of electrical activity at cell membranes interacting with self-generated and externally imposed electric fields, J. Neural Eng., 10 (2013), 026019.
- [2] D. N. ARNOLD, R. S. FALK, AND R. WINTHER, Multigrid in H(div) and H(curl), Numer. Math., 85 (2000), pp. 197–217.
- [3] W. M. Boon, M. Hornkjøl, M. Kuchta, K.-A. Mardal, and R. Ruiz-Baier, Parameterrobust methods for the Biot-Stokes interfacial coupling without Lagrange multipliers, J. Comput. Phys., 467 (2022), 111464.
- [4] J. H. BRAMBLE, Multigrid Methods, Pitman Research Notes in Mathematics Series 294, Longman Scientific & Technical, Harlow, UK, 1993.

- [5] M. Brezina, R. Falgout, S. MacLachlan, T. Manteuffel, S. McCormick, and J. Ruge, Adaptive smoothed aggregation (αSA) multigrid, SIAM Rev., 47 (2005), pp. 317–346, https://doi.org/10.1137/050626272.
- [6] A. P. Buccino, M. Kuchta, K. H. Jæger, T. V. Ness, P. Berthet, K.-A. Mardal, G. Cauwenberghs, and A. Tveito, How does the presence of neural probes affect extracellular potentials?, J. Neural Eng., 16 (2019), 026030, https://doi.org/10.1088/1741-2552/ab03a1.
- [7] A. P. BUCCINO, M. KUCHTA, J. SCHREINER, AND K.-A. MARDAL, Improving Neural Simulations with the EMI Model, Springer International Publishing, Cham, Switzerland, 2021, pp. 87–98, https://doi.org/10.1007/978-3-030-61157-6\_7.
- [8] A. Budiša, X. Hu, M. Kuchta, K.-A. Mardal, and L. T. Zikatanov, HAZniCS software components for multiphysics problems, ACM Trans. Math. Softw., 49 (2023), 36, https://doi.org/10.1145/3625561.
- [9] D. CERRONI, F. LAURINO, AND P. ZUNINO, Mathematical analysis, finite element approximation and numerical solvers for the interaction of 3d reservoirs with 1d wells, GEM Int. J. Geomath., 10 (2019), pp. 1–27.
- [10] M. CORTI, P. F. ANTONIETTI, L. DEDE, AND A. M. QUARTERONI, Numerical modeling of the brain poromechanics by high-order discontinuous Galerkin methods, Math. Models Methods Appl. Sci., 33 (2023), pp. 1577–1609, https://doi.org/10.1142/S0218202523500367.
- [11] P. D'AMBRA, F. DURASTANTE, S. FILIPPONE, AND L. ZIKATANOV, Automatic coarsening in Algebraic Multigrid utilizing quality measures for matching-based aggregations, Comput. Math. Appl., 144 (2023), pp. 290–305, https://doi.org/10.1016/j.camwa.2023.06.026.
- [12] P. D'Ambra and P. S. Vassilevski, Adaptive AMG with coarsening based on compatible weighted matching, Comput. Vis. Sci., 16 (2013), pp. 59–76, https://doi.org/10.1007/ s00791-014-0224-9.
- [13] C. D'ANGELO AND A. QUARTERONI, On the coupling of 1d and 3d diffusion-reaction equations: Application to tissue perfusion problems, Math. Models Methods Appl. Sci., 18 (2008), pp. 1481–1504.
- [14] T. A. DAVIS, Algorithm 832: UMFPACK V4.3—An unsymmetric-pattern multifrontal method, ACM Trans. Math. Software, 30 (2004), pp. 196–199.
- [15] R. W. Dos Santos, G. Plank, S. Bauer, and E. J. Vigmond, Parallel multigrid preconditioner for the cardiac bidomain model, IEEE Trans. Biomed. Eng., 51 (2004), pp. 1960–1968.
- [16] P. E. FARRELL, M. G. KNEPLEY, L. MITCHELL, AND F. WECHSUNG, PCPATCH: Software for the topological construction of multigrid relaxation methods, ACM Trans. Math. Software, 47 (2021), pp. 1–22.
- [17] P. C. FRANZONE, L. F. PAVARINO, AND S. SCACCHI, Mathematical Cardiac Electrophysiology, MS&A 13, Springer-Verlag, Berlin, 2014.
- [18] I. G. GJERDE, K. KUMAR, AND J. M. NORDBOTTEN, A singularity removal method for coupled 1d-3d flow models, Comput. Geosci., 24 (2020), pp. 443-457.
- [19] F. Goirand, T. Le Borgne, and S. Lorthois, Network-driven anomalous transport is a fundamental component of brain microvascular dysfunction, Nat. Commun., 12 (2021), 7295.
- [20] M. GRIEBEL AND P. OSWALD, On the abstract theory of additive and multiplicative Schwarz algorithms, Numer. Math., 70 (1995), pp. 163–180, https://doi.org/10.1007/s002110050115.
- [21] G. Hartung, S. Badr, S. Mihelic, A. Dunn, X. Cheng, S. Kura, D. A. Boas, D. Kleinfeld, A. Alaraj, and A. A. Linninger, Mathematical synthesis of the cortical circulation for the whole mouse brain—Part II: Microcirculatory closure, Microcirculation, 28 (2021), e12687.
- [22] E. HODNELAND, X. Hu, and J. M. Nordbotten, Well-posedness and discretization for a class of models for mixed-dimensional problems with high-dimensional gap, SIAM J. Appl. Math., 81 (2021), pp. 2218–2245.
- [23] Q. Hong, J. Kraus, M. Lymbery, and F. Philo, Conservative discretizations and parameterrobust preconditioners for Biot and multiple-network flux-based poroelasticity models, Numer. Linear Algebra Appl., 26 (2019), e2242.
- [24] Q. Hong, J. Kraus, M. Lymbery, and F. Philo, Parameter-robust Uzawa-type iterative methods for double saddle point problems arising in Biot's consolidation and multiple-network poroelasticity models, Math. Models Methods Appl. Sci., 30 (2020), pp. 2523–2555.
- [25] X. Hu, E. Keilegavlen, and J. M. Nordbotten, Effective preconditioners for mixeddimensional scalar elliptic problems, Water Resour. Res., 59 (2023), e2022WR032985.

- [26] X. Hu and P. S. Vassilevski, Modifying AMG coarse spaces with weak approximation property to exhibit approximation in energy norm, SIAM J. Matrix Anal. Appl., 40 (2019), pp. 1131–1152, https://doi.org/10.1137/18M1165190.
- [27] N. M. M. HUYNH, F. CHEGINI, L. F. PAVARINO, M. WEISER, AND S. SCACCHI, Convergence analysis of BDDC preconditioners for composite DG discretizations of the cardiac cell-bycell model, SIAM J. Sci. Comput., 45 (2023), pp. A2836–A2857.
- [28] N. M. M. HUYNH, L. F. PAVARINO, AND S. SCACCHI, Scalable and robust dual-primal Newton– Krylov deluxe solvers for cardiac electrophysiology with biophysical ionic models, Vietnam J. Math., 50 (2022), pp. 1029–1052.
- [29] H. KIM, J. XU, AND L. ZIKATANOV, A multigrid method based on graph matching for convection-diffusion equations, Numer. Linear Algebra Appl., 10 (2003), pp. 181–195, https://doi.org/10.1002/nla.317.
- [30] T. KÖPPL, E. VIDOTTO, B. WOHLMUTH, AND P. ZUNINO, Mathematical modeling, analysis and numerical approximation of second-order elliptic problems with inclusions, Math. Models Methods Appl. Sci., 28 (2018), pp. 953–978.
- [31] M. Kuchta, Assembly of multiscale linear PDE operators, in Numerical Mathematics and Advanced Applications ENUMATH 2019: European Conference, Egmond aan Zee, Netherlands, Springer-Verlag, Berlin, 2020, pp. 641–650.
- [32] M. KUCHTA, F. LAURINO, K.-A. MARDAL, AND P. ZUNINO, Analysis and approximation of mixed-dimensional PDEs on 3D-1D domains coupled with Lagrange multipliers, SIAM J. Numer. Anal., 59 (2021), pp. 558–582.
- [33] M. KUCHTA, K.-A. MARDAL, AND M. MORTENSEN, Preconditioning trace coupled 3d-1d systems using fractional Laplacian, Numer. Methods Partial Differential Equations, 35 (2019), pp. 375–393.
- [34] F. LAURINO AND P. ZUNINO, Derivation and analysis of coupled PDEs on manifolds with high dimensionality gap arising from topological model reduction, ESAIM Math. Model. Numer. Anal., 53 (2019), pp. 2047–2080.
- [35] Y.-J. LEE, J. WU, J. XU, AND L. ZIKATANOV, Robust subspace correction methods for nearly singular systems, Math. Models Methods Appl. Sci., 17 (2007), pp. 1937–1963.
- [36] Y.-J. LEE, J. WU, J. XU, AND L. ZIKATANOV, Robust subspace correction methods for nearly singular systems, Math. Models Methods Appl. Sci., 17 (2007), pp. 1937–1963, https://doi.org/10.1142/S0218202507002522.
- [37] Y.-J. LEE, J. Wu, J. Xu, and L. Zikatanov, A sharp convergence estimate for the method of subspace corrections for singular systems of equations, Math. Comp., 77 (2008), pp. 831–850, https://doi.org/10.1090/S0025-5718-07-02052-2.
- [38] A. LINNINGER, G. HARTUNG, S. BADR, AND R. MORLEY, Mathematical synthesis of the cortical circulation for the whole mouse brain—Part I. Theory and image integration, Comput. Biol. Med., 110 (2019), pp. 265–275.
- [39] O. LIVNE AND A. BRANDT, Lean algebraic multigrid (LAMG): Fast graph Laplacian linear solver, SIAM J. Sci. Comput., 34 (2012), pp. 499–523.
- [40] A. LOGG, K.-A. MARDAL, AND G. WELLS, Automated Solution of Differential Equations by the Finite Element Method, Lect. Notes Comput. Sci. Engrg. 84, Springer Science & Business Media, New York, 2012.
- [41] NeuroMorpho.Org, Digital reconstruction of a neuron, ID NMO-129521, 2020, https://neuromorpho.org/neuron\_info.jsp?neuron\_name=PolyIC\_3AS2\_1.
- [42] L. F. PAVARINO AND S. SCACCHI, Multilevel additive Schwarz preconditioners for the bidomain reaction-diffusion system, SIAM J. Sci. Comput., 31 (2008), pp. 420–443.
- [43] D. W. Peaceman, Interpretation of well-block pressures in numerical reservoir simulation (includes associated paper 6988), Soc. Petrol. Eng. J., 18 (1978), pp. 183–194.
- [44] M. Pennacchio and V. Simoncini, Algebraic multigrid preconditioners for the bidomain reaction-diffusion system, Appl. Numer. Math., 59 (2009), pp. 3033-3050.
- [45] E. PIERSANTI, J. J. LEE, T. THOMPSON, K.-A. MARDAL, AND M. E. ROGNES, Parameter robust preconditioning by congruence for multiple-network poroelasticity, SIAM J. Sci. Comput., 43 (2021), pp. B984–B1007.
- [46] E. PIERSANTI, M. E. ROGNES, AND K.-A. MARDAL, Parameter robust preconditioning for multicompartmental Darcy equations, in Numerical Mathematics and Advanced Applications ENUMATH 2019: European Conference, Egmond aan Zee, Netherlands, Springer-Verlag, Berlin, 2020, pp. 703-711.
- [47] F. RATHGEBER, D. A. HAM, L. MITCHELL, M. LANGE, F. LUPORINI, A. T. T. MCRAE, G.-T. BERCEA, G. R. MARKALL, AND P. H. J. KELLY, Firedrake: Automating the finite element method by composing abstractions, ACM Trans. Math. Software, 43 (2016), pp. 1–27.

- [48] J. SCHÖBERL, Multigrid methods for a parameter dependent problem in primal variables, Numer. Math., 84 (1999), pp. 97–119.
- [49] A. SINCLAIR AND M. JERRUM, Approximate counting, uniform generation and rapidly mixing Markov chains, Inform. and Comput., 82 (1989), pp. 93–133, https://doi.org/10.1016/ 0890-5401(89)90067-9.
- [50] J. G. STINSTRA, C. HENRIQUEZ, AND R. MACLEOD, Comparison of microscopic and bidomain models of anisotropic conduction, in 2009 36th Annual Computers in Cardiology Conference (CinC), IEEE, New York, 2009, pp. 657–660.
- [51] J. SUNDNES, G. T. LINES, X. CAI, B. F. NIELSEN, K.-A. MARDAL, AND A. TVEITO, Computing the Electrical Activity in the Heart, Monogr. Comput. Sci. Engrg. 1, Springer Science & Business Media, New York, 2007.
- [52] J. SUNDNES, B. F. NIELSEN, K. A. MARDAL, X. CAI, G. T. LINES, AND A. TVEITO, On the computational complexity of the bidomain and the monodomain models of electrophysiology, Ann. Biomed. Eng., 34 (2006), pp. 1088–1097.
- [53] A. TOSELLI AND O. WIDLUND, Domain Decomposition Methods—Algorithms and Theory, Springer Series in Computational Mathematics 34, Springer-Verlag, Berlin, 2005.
- [54] L. Tung, A Bi-domain Model for Describing Ischemic Myocardial D-C Potentials, Ph.D. thesis, Massachusetts Institute of Technology, 1978.
- [55] A. TVEITO, K. H. JÆGER, M. KUCHTA, K.-A. MARDAL, AND M. E. ROGNES, A cell-based framework for numerical modeling of electrical conduction in cardiac tissue, Front. Phys., 5 (2017), 48.
- [56] P. Vaněk, J. Mandel, and M. Brezina, Algebraic multigrid by smoothed aggregation for second and fourth order elliptic problems, Computing, 56 (1996), pp. 179–196, https:// doi.org/10.1007/BF02238511.
- [57] P. VASSILEVSKI, Multilevel Block Factorization Preconditioners: Matrix-Based Analysis and Algorithms for Solving Finite Element Equations, Springer-Verlag, Berlin, 2008, http://www.springer.com/mathematics/computational+science+%26+engineering/book/978-0-387-71563-6.
- [58] A. J. WATHEN, Realistic eigenvalue bounds for the Galerkin mass matrix, IMA J. Numer. Anal., 7 (1987), pp. 449–457.
- [59] J. Xu, Iterative methods by space decomposition and subspace correction, SIAM Rev., 34 (1992), pp. 581-613, https://doi.org/10.1137/1034116.
- [60] J. Xu and L. Zikatanov, The method of alternating projections and the method of subspace corrections in Hilbert space, J. Amer. Math. Soc., 15 (2002), pp. 573–597, https://doi.org/ 10.1090/S0894-0347-02-00398-3.
- [61] J. Xu And L. Zikatanov, Algebraic multigrid methods, Acta Numer., 26 (2017), pp. 591–721, https://doi.org/10.1017/S0962492917000083.
- [62] S. ZAMPINI, Dual-primal methods for the cardiac bidomain model, Math. Models Methods Appl. Sci., 24 (2014), pp. 667–696.
- [63] L. T. ZIKATANOV, Two-sided bounds on the convergence rate of two-level methods, Numer. Linear Algebra Appl., 15 (2008), pp. 439–454, https://doi.org/10.1002/nla.556.